Efficient Slurry-Phase Homopolymerization of Ethylene to Branched Polyethylenes Using α-Diimine Nickel(II) Catalysts Covalently Linked to Silica Supports

Henri S. Schrekker,*,† Vasily Kotov, Peter Preishuber-Pflugl, Peter White, and Maurice Brookhart*

Department of Chemistry, University of North Carolina at Chapel Hill, Chapel Hill, North Carolina 27599-3290

Received May 8, 2006; Revised Manuscript Received July 17, 2006

ABSTRACT: α-Diimine nickel(II) complexes covalently linked to a silica support were obtained by the reaction of an amino- or hydroxy-functionalized α-diimine nickel complex with silica particles treated with trimethyl aluminum. These silica-supported aryl α-diimine nickel(II) precatalysts linked via an amino (**1a**) or hydroxy functionality (**1b**−**c**) at the *p*-aryl position, and precatalysts linked via one (**2a**) or two (**2b**) hydroxy functionalities in the alkyl backbone were used in slurry polymerizations of ethylene to produce branched polyethylenes. Activation of precatalysts with ethylaluminum sesquichloride was effective even at very low Al/Ni ratios of 48. Initial polymerizations, performed at 60 °C and 150 psig ethylene, showed excellent productivities of up to 10.8 kg PE per gram of **1b** (3.0 wt % nickel loading). Low productivities at temperatures above 60 °C can in part be overcome by increase in ethylene pressure. For example, a productivity of 6.0 kg PE per gram of **1b** (3.0 wt % nickel loading) was obtained at 80 °C and 700 psig ethylene. The best polymerization productivities were obtained with trimethylaluminum as a traceless silica-linker, however, tetrachlorosilane and trichloroborane are attractive alternatives. Branching densities can be controlled by choice of *ortho*-aryl substituents. No reactor fouling occurs with these supported catalysts.

Introduction

The demand for polyethylenes (PEs) is enormous due to numerous end applications in bulk products.[1−3] Transformation of the PE industry into a multibillion dollar a year business[4,5] started with the discovery of heterogeneous titanium catalysts by Ziegler in the mid 1950s.[6−8] Production of PEs is still dominated by coordination-insertion catalysts based on early transition metals. Coordination polymerization technologies of supported titanium (Ziegler−Natta)[8−10] and chromium (Phillips and Union Carbide)[11,12] catalysts are used for the production of high-density polyethylene (HDPE), a linear semicrystalline ethylene homopolymer ($T_m \sim 136$ °C).[13] Linear low-density polyethylenes (LLDPEs) are random copolymers of ethylene and an α-olefin exhibiting a range of T_m's below 130 °C[13] prepared using Ziegler−Natta,[8] chromium,[11] or metallocene catalysts.[4,14−17] An alternative technique for the synthesis of LLDPE combines an ethylene oligomerization catalyst with a catalyst that copolymerizes the in situ produced α-olefins with ethylene.[7,18−20] Such a dual catalyst system was described by Phillips for the production of a hexene−ethylene copolymer.[21] A disadvantage of this general approach is that α-olefin residues can be present in the copolymer due to an incomplete incorporation. Low-density polyethylene (LDPE, $T_m = 100-115$ °C)[13] is a homopolymer exhibiting branches of variable length, which is produced via a radical chain growth process at high temperatures and high ethylene pressures (15 000−45 000 psig ethylene at 120−300 °C).[22]

* Corresponding authors. E-mail: schrekker@iq.ufrgs.br (H.S.S.); mbrookhart@unc.edu (M.B.). Telephone: +55-51-3316-6284 (H.S.S); +1-919-962-0362 (M.B.). Fax: +55-51-3316-7304 (H.S.S); +1-919-962-2476 (M.B.).

† Current address: Institute of Chemistry, Universidade Federal do Rio Grande do Sul, Av. Bento Gonçalves 9500, Porto Alegre, RS, CEP 91501-970, Brazil.

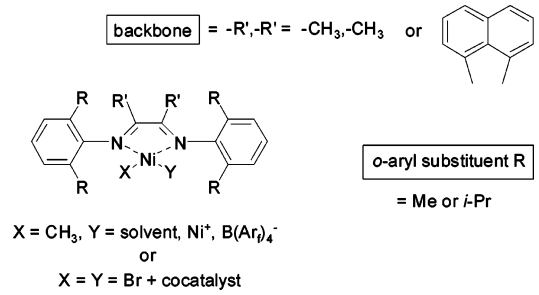

Figure 1. General structure of α-diimine nickel(II) catalysts.

In general, ethylene insertion rates for late transition metal catalysts are lower than those of early transition metal catalysts[23,24] and β-hydride elimination leading to chain transfer competes with chain growth, resulting in the formation of short-chain oligomers.[25] This chemistry forms the basis of the Shell higher olefin process (SHOP) for production of α-olefins from ethylene using neutral nickel catalysts containing bidentate oxygen−phosphorus ligands.[26−28] Certain nickel(II) complexes containing modified SHOP ligands show moderate activity for forming linear PE.[18]

A breakthrough in Ni-catalyzed ethylene polymerization chemistry came in 1995 when this group reported the discovery of *ortho*-substituted aryl α-diimine nickel(II) and palladium(II) catalysts (Figure 1) for the synthesis of high-molecular-weight branched PE.[18,24,29−33] Following this discovery, collaborative efforts of the UNC and DuPont groups led to expansion of this catalyst family, which is now part of the Versipol polymerization catalyst technology from DuPont.[34]

In the nickel and palladium diimine systems, the aryl groups are oriented perpendicular to the ligand coordination plane, and introduction of substituents in the *ortho*-aryl positions provides steric bulk above and below the square planar metal center and

10.1021/ma061032v CCC: $33.50
Published on Web 08/25/2006

Scheme 1. Chain Walking (*P* = growing polymer chain).[18,29,45−47]

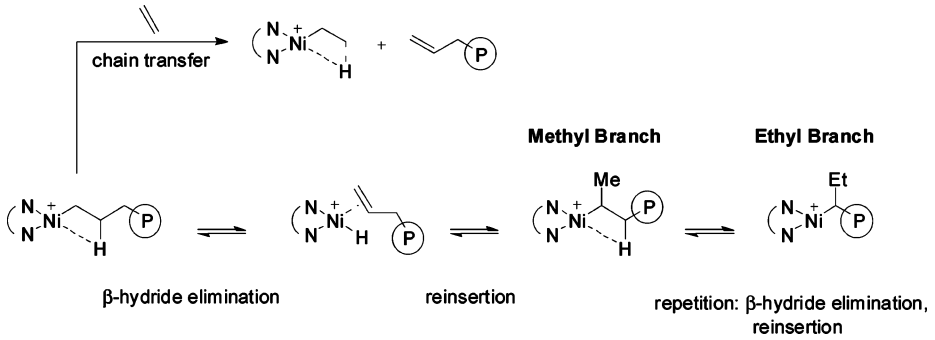

thus retards chain transfer (Scheme 1).[29,30] Chain growth is now favored over chain transfer, which results in a dramatic change from low- to high-molecular-weight PE.[29] A similar ligand design was incorporated into the bis(imino) pyridyl iron and cobalt catalysts, which yield high-molecular-weight PE.[18,35−39] Ethylene polymerization activity of the nickel catalysts is extremely high as a consequence of the highly electrophilic nature of the cationic nickel center, which lowers the migratory insertion barrier of ethylene into the growing polymer chain.[29,40] Cationic palladium(II) analogues are much less reactive due to their reduced electrophilicity.[18,29] The bis(imino) pyridyl iron catalysts are interesting due to their thermal stability, and high activities are obtained even at temperatures above 100 °C.[35] However, ethylene polymerization with these catalysts affords HDPE.[35,41] A unique feature of the α-diimine nickel(II) and palladium(II) catalysts is that branched PE is obtained in ethylene homopolymerizations.[18,29] Highly branched, completely amorphous PE is normally obtained with the palladium catalysts.[29,42] α-Diimine nickel(II) catalysts produce PE with branching levels of 5−100 branches per 1000 carbons depending on ligand structure and reaction conditions, which corresponds to melting points between 25 and 135 °C.[29,30] The types of branches obtained vary from mainly methyl to ethyl and higher aliphatic chains, and branches on branches are observed.[18,43,44] A "chain-walking" mechanism, which involves sequential *β*-hydride elimination and reinsertion reactions, is responsible for the branching (Scheme 1).[18,29,45−47] In general, the PE microstructure can be predictably modified by altering the steric bulk of the *ortho*-aryl substituents, ethylene pressure, and reaction temperature.[30,48] Branching densities increase with an increase in steric bulk of the *ortho* substituents, with an increase in temperature and with a decrease in pressure. These unique properties of the α-diimine nickel(II) catalysts make this technology a potentially attractive alternative for the production of LDPE. Branching levels go far beyond what is possible in the free radical polymerizations, thus a wider range of PE properties are available using these catalysts.

Gas-phase and slurry-phase polymerization processes employing titanium or chromium catalysts are the principal commercial methods for production of polyethylenes via metal catalysis.[8−12] Using nickel diimine catalysts in either of these commercial processes presents challenges, in large part due to the deactivation of these catalysts at high temperatures.[18] Because slurry-phase polymerizations can be run at moderate temperatures of 70−90 °C, this process is more attractive for use with the nickel catalysts. Ideally a "drop-in" catalyst system might be developed which could be utilized in existing slurry facilities.

A common approach to developing catalysts for use in slurry processes is to heterogenize effective homogeneous catalysts by immobilizing them on solid supports.[8,49−51] Mesoporous silica particles are frequently chosen as the support material due to their excellent fragmentation properties, which allows growth of the particles together with good control of the exotherm.[8,49−51] A typical approach for generating the supported catalyst involves, first, treatment of the silica particles with methyl aluminoxane (MAO) to form surface-bound MAO, followed by treatment of these particles with an early metal precatalyst.[52] The MAO serves to convert the precatalyst to the active cationic metal alkyl complex, which is anchored to the particle through the ionic attraction to the surface-bound anions (electrostatic interactions). Under ideal circumstances, as ethylene is taken up, these particles grow and fragment; the morphology of the original particle is reproduced and no reactor fouling occurs. An attractive feature of this method is that no modification of the catalyst is required for "attachment" to the support.

On the basis of patent disclosures and publications, translation of this technique to the α-diimine Ni(II) catalysts is not entirely satisfactory. Heterogenized catalysts were obtained by addition of Ni(II) diimine complexes to MAO-treated silica[53−55] or, alternatively, by reaction of the diimine complexes with MAO prior to addition to the silica support (Figure 2).[56] The following limitations of this technique were observed: (1) a limited loading capacity of the nickel catalysts, (2) agglomeration of PE on the reactor wall due to leaching of α-diimine nickel(II) catalysts from the silica support, and (3) significantly reduced productivities when compared to the homogeneous polymerizations (Figure 2). When performed under the same polymerization conditions, the productivity per gram of nickel decreased from 250−450 kg PE for the homogeneous polymerization to 50 kg PE for the silica-MAO supported catalysts. Furthermore, the productivity per gram of supported catalyst is quite low, which can in part be ascribed to catalyst deactivation as well as low loading capacity of the silica using this technique. Large molar excesses of MAO are used to support and activate the α-diimine nickel(II) catalysts. Excess MAO might be responsible for the reduction and, as a consequence, deactivation of the catalyst.[57,58] However, little is known about the deactivation of these catalysts.

Covalent attachment of the α-diimine nickel(II) precatalyst to a support would offer a choice of the alkyl aluminum cocatalyst to be used and better control of the cocatalyst amount (Figure 2). One way to achieve this is to first support the α-diimine ligand and then treat this system with $NiBr_2$(1,2-dimethoxyethane) to form the supported α-diimine nickel(II) dibromide precatalyst.[59−61] Boussie used this method in which diimine ligands were bound to a polystyrene support for the discovery of new α-diimine nickel(II) catalysts in a combinatorial fashion.[62] Another example employing this method involved the covalent attachment of diimines to silica via a siloxane linkage.[63] A general disadvantage of this strategy is that the formation of the nickel(II) complex is not always

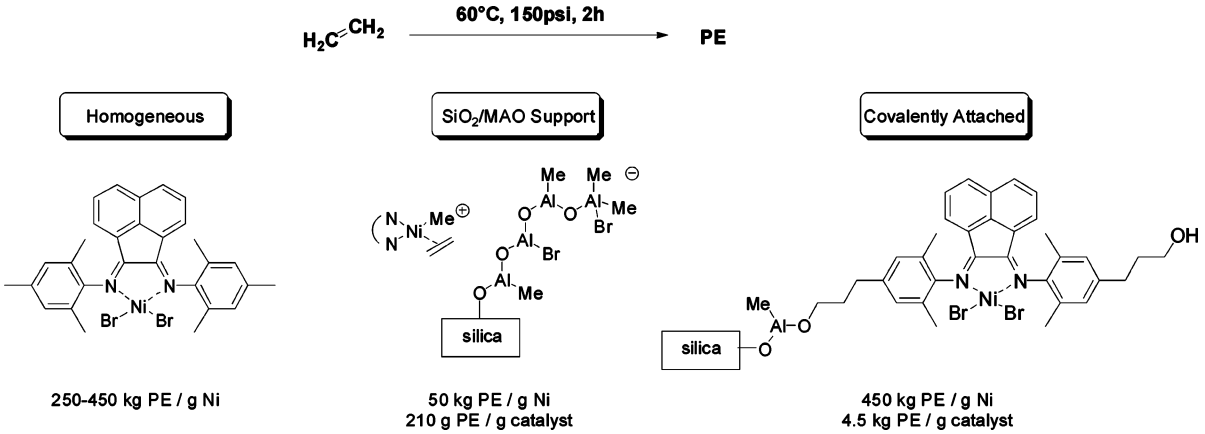

Figure 2. Comparison of homogeneous vs heterogenized α-diimine nickel(II) catalysts.

Scheme 2. General Approach for the Synthesis of Silica-Supported α-Diimine Nickel(II) Catalysts via a Covalent Attachment.

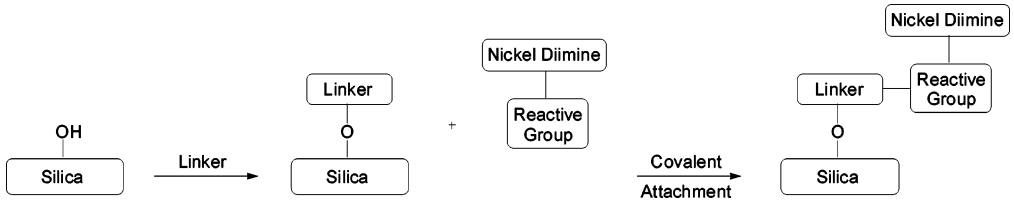

straightforward and will be even more complicated when performed on a solid support. The determination of precise nature of the supported catalysts is problematic.

Formation of the α-diimine nickel(II) complexes prior to attachment to the support circumvents these problems and allows a reliable strategy for the synthesis of supported α-diimine nickel(II) catalysts. Such a strategy has previously been used for supporting SHOP-type oligomerization catalysts.[64] Recently, Herrmann reported bis(imino) pyridyl iron(II) ethylene polymerization catalysts covalently linked to silica prepared via hydrosilation of the alkenyl-functionalized iron(II) complexes by a functionalized silica support.[65] In work patented by Repsol,[66] Mendez Llatas et al., reported attachment of $[ArN{=}C(R^1){-}C(R^2){=}NAr]NiBr_2$ (Ar = 2,6-$Me_2C_6H_3$− or 2,6-*i*-$Pr_2C_6H_3$−, R^1 = $-CH_3$ or $-CH_2CH_2CH_2Si(OCH_3)_3$, R^2 = $-CH_2CH_2CH_2Si(OCH_3)_3$) to mesoporous silica particles via Si−O linkages formed from elimination of MeOH. When activated with MAO, these catalysts exhibited low productivities in the range of 0.01−0.09 kg PE per gram of supported catalyst at 45−60 °C. Previously, we reported a new methodology for the covalent attachment of α-diimine nickel(II) complexes to a silica support (Scheme 2).[67,68] α-Diimine nickel(II) complexes which contain an amino or hydroxy functionality were reacted with trimethylaluminum (TMA)-treated silica to afford the covalently linked catalysts. Activation of these precatalysts with an alkylaluminum cocatalyst afforded a highly productive ethylene polymerization system. Note that nearly the same productivity per gram of nickel is observed as in the homogeneous system, and an excellent productivity of 4.5 kg PE per gram of supported precatalyst is obtained (Figure 2). Herein we report our results regarding optimization of (1) the polymerization procedure, (2) the α-diimine nickel(II) catalysts, (3) the silica-linker, (4) the polymerization temperature, (5) the ethylene pressure, and (6) the nickel load of the α-diimine nickel(II) complex on the silica support in slurry polymerizations of ethylene. These detailed investigations were performed to obtain better productivities at elevated temperatures of 80 °C or higher and to realize control of the polymer properties with the goal of developing this technology to be competitive for the production of LDPE and related lower-density polyethylenes.

Scheme 3. Synthesis of α-Diimine Ligands with an Amino or Hydroxy Functionality Attached to the *Para*-Aryl Position.

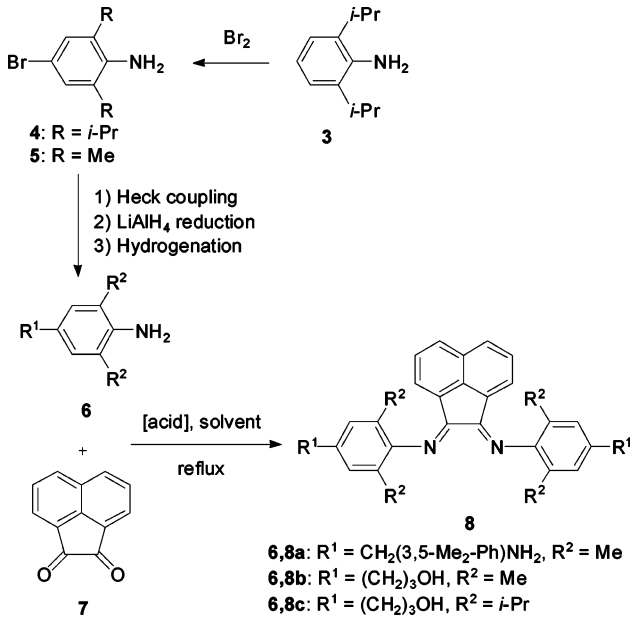

Results and Discussion

Ligand Synthesis. The highly active silica-supported aryl α-diimine nickel(II) catalysts previously reported by us contained either an amino or hydroxy functionality at the *para*-aryl position, which allowed a covalent attachment to the silica support.[67] Synthesis of the corresponding aryl α-diimine ligands is achieved by the reaction of the functionalized aniline with acenaphthenequinone (Scheme 3). In our initial studies, we examined *ortho*,*ortho*-dimethyl-substituted anilines, as these are easily accessible, which allowed the comparison of various amino- and hydroxyl-substituted ligand systems. The sulfuric acid-catalyzed condensation reaction of aniline **6a** with acenaph-

Scheme 4. Synthesis of α-Diimine Ligands with a Hydroxy Functionality Attached to the Backbone.

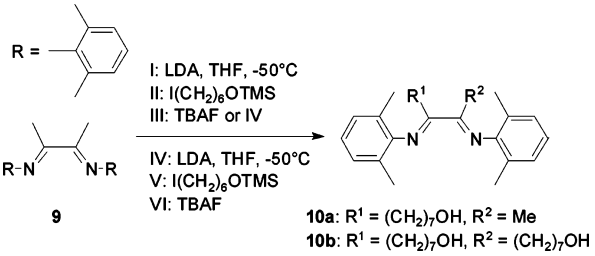

thenequinone afforded amino-functionalized α-diimine **8a** in a moderate yield of 62%. Introduction of a hydroxyl functionality was accomplished starting from bromoaniline **5**. A palladium-catalyzed Heck coupling with methylacrylate, followed by a lithium aluminum hydride reduction of the ester and hydrogenation with palladium on activated carbon, afforded hydroxy-functionalized aniline **6b** in an overall yield of 22%. This strategy allows facile variation of the *ortho*-aryl substituents, and diisopropylaniline **6c** was synthesized in an overall yield of 18% from aniline **3**. The acid-catalyzed condensation reaction of anilines **6b** and **6c** with acenaphthenequinone afforded the hydroxy-functionalized α-diimine ligands **8b** and **8c** in 66 and 48% unoptimized yields, respectively.[69]

The synthesis of α-diimine ligands with a hydroxy functionality attached to the backbone is presented in Scheme 4. Attachment of one or two hydroxyl tails to the dimethyl backbone of α-diimine **9** is easily achieved by a proper choice of the reaction conditions. Treatment of α-diimine **9** with lithium diisopropylamine and 1 equivalent TMS-protected iodohexanol introduces the first hydroxy-tail; the second one can be introduced by a consecutive addition of lithium diisopropylamine and another equivalent of TMS-protected iodohexanol. Deprotection after the first or second step with tetrabutylammonium fluoride affords either monohydroxy α-diimine **10a** or dihydroxy α-diimine **10b** in yields of 82 or 65%, respectively.

Synthesis $NiBr_2$ Complexes. A previously described procedure was used for the synthesis of α-diimine nickel(II) bromide complexes **11a−c** and **12a,b** (Scheme 5).[30,67] No protective groups for the amino and hydroxy functionalities are needed, and reaction of the α-diimine ligands with $NiBr_2$(1,2-dimethoxyethane) resulted generally in excellent yields. Yields of complexes **11c** and **12b** were somewhat low due to good solubility of these complexes in the solvents used for purification. Suitable crystals for X-ray analysis were obtained for α-diimine nickel(II) bromide **12a** (Figure 3). The X-ray analysis confirms the assigned structure of **12a**. As expected for the dibromide, tetrahedral coordination of Ni(II) is observed. The aryl groups lie perpendicular to the plane of α-diimine ligand, and the *ortho*-methyl substituents are located above and below this plane.

Synthesis of Precatalysts. Covalent attachment of α-diimine nickel(II) complexes requires the treatment of the silica support

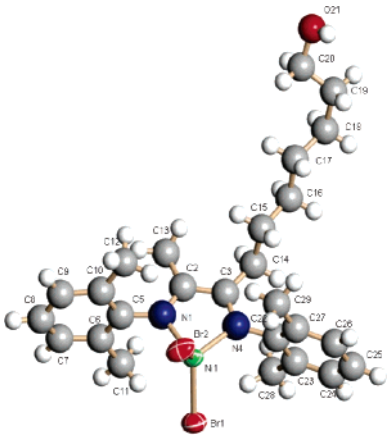

Figure 3. ORTEP view of α-diimine nickel(II) bromide **12a**. Selected interatomic distances (Å): Ni(1)−Br(1) 2.331, Ni(1)−Br(2) 2.338, Ni-(1)−N(1) 2.021, N(1)−C(2) 1.304, C(2)−C(3) 1.477, C(3)−N(4) 1.360, Ni(1)−N(4) 1.991. Selected angles (deg): Br(1)−Ni(1)−Br(2) 121.31, N(1)−Ni(1)−N(4) 80.07, Ni(1)−N(1)−C(2) 115.03, N(1)−C(2)−C(3) 116.25, C(2)−C(3)−N(4) 112.70, C(3)−N(4)−Ni(1) 115.83, C(2)−N(1−C(5) 123.38, C(3)−N(4)−C(22) 121.67. Selected torsion angles (deg): C(2)−N(1)−C(5)−C(6) 94.31, C(2)−N(1)−C(5)−C(10) −86.97.

with a linker (Scheme 6). Grace Davison silicas XPO-2402 and SP9-496 were treated with an excess of TMA, or $SiCl_4$, or BCl_3, which results either in the release of methane or hydrogen chloride. Reaction of the α-diimine nickel(II) complexes **11a−c** and **12a,b** with these activated silica supports **14** afforded the desired covalent attachment with release of methane with support **14a** or hydrogen chloride with the supports **14b,c** (Scheme 6). It is unknown whether one or both of the functionalities are linked to the silica support in the case of precatalysts **1a−c** and **2b**. High nickel loadings of up to 3.0 wt % were achieved with this strategy in quantitative yields for the α-diimine nickel(II) precatalysts **1a−c** and **2a,b**.

Determination of the nickel loading on the silica-supported precatalyst is important for determining the productivity per gram of nickel. Values reported in our previous communication were found by an ICP-OES analysis of the silica-supported precatalyst.[67] Since this report, we have discovered that this analytical technique resulted consistently in low estimates of nickel loading. For instance, preparation of silica-supported precatalyst **1b1** with a 1.0 wt % nickel loading by the treatment of activated silica **14a** with a dichloromethane solution of α-diimine nickel(II) complex **11b** resulted in *complete* decoloration of the brown dichloromethane solution while the silica particles acquired a brown color. However, a nickel loading of 0.6 wt % was found by ICP-OES analysis. In this work, nickel loadings were determined by analysis of the nickel content left in the dichloromethane solution following supportation as determined by ICP-OES. The nickel loadings determined were in all instances only slightly below the theoretical maximum nickel loading. (If some insoluble (ligand) $NiBr_2$ remains in the dichloromethane solution and is filtered off, a high estimate of

Scheme 5. Synthesis of α-Diimine $NiBr_2$ complexes.

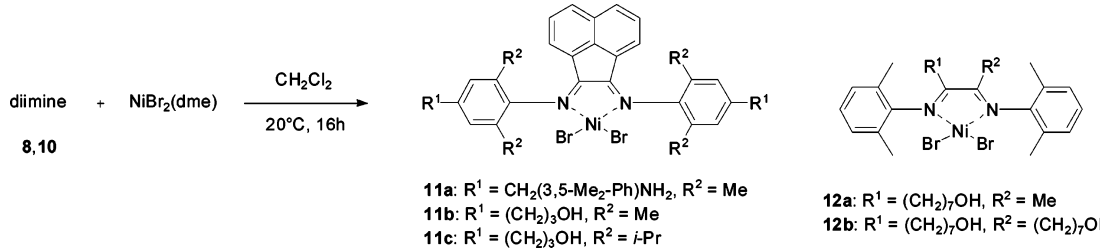

Scheme 6. Preparation of Silica-Supported α-Diimine Nickel(II) Precatalysts.

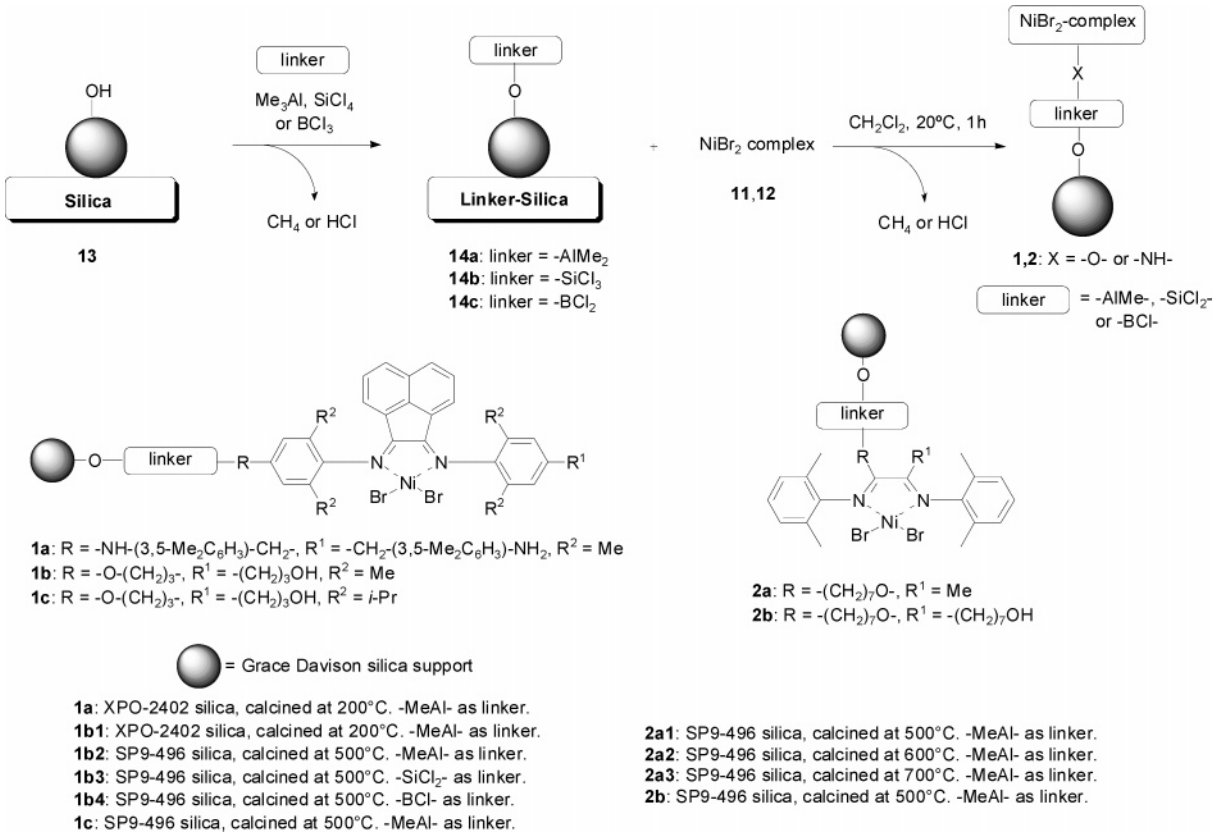

Table 1. Ethylene Slurry Polymerizations Employing Precatalysts 1b1 and 1b2

$H_2C{=}CH_2$ —(10 mg precatalyst 1b1 or 1b2; 100 mL pentane, 150 psig ethylene)→ PE

1b1: Grace Davison XPO-2402, calcined at 200°C, -MeAl- as linker.
1b2: Grace Davison SP9-496, calcined at 500°C, -MeAl- as linker.

entry	precat[a]	wt % Ni[b]	*T* [°C]	time [h]	cocat[c]	Al:Ni	proc[d]	kg PE/ g **1b1**/**2**	kg PE/ g Ni	T_m [°C][e]	M_w[f] [g/mol]	PDI [f]	branches/ 1000C[g]
1	**1b2**	1.0	60	1	none	214	3	0	0				
2	**1b1**	1.0	60	2	EASC	420	1b	4.5	450[h]	126	131k	3.3	13
3	**1b1**	1.0	60	2	EASC	48	1b	4.3	430[h]	n.d.	n.d.	n.d.	n.d.
4	**1b1**	3.0	60	2	EASC	330	1b	10.8	350[h]	125	136k	3.4	14
5	**1b1**	1.0	80	2	EASC	480	1b	1.2	120[h]	122	74k	3.5	n.d.
6	**1b1**	1.0	60	2	MADC	480	1b	3.9	390[h]	127	131k	3.4	n.d.
7	**1b1**	1.0	80	2	MADC	480	1b	1.7	170[h]	121	73k	3.7	n.d.
8	**1b2**	1.0	60	1	EASC	214	3	2.8	279	126	148k	5.4	n.d.
9	**1b2**	1.0	60	2	EASC	214	3	3.3	334	125	155k	5.2	22
10	**1b2**	1.0	60	2	EASC	214	1a	2.8	284	126	149k	8.2	n.d.
11	**1b2**	1.0	60	2	EASC	214	2	3.0	301	127	157k	6.0	n.d.

[a] Precatalyst. [b] Theoretical maximum nickel loading. [c] Cocatalyst: EASC = $Et_3Al_2Cl_3$; MADC = $Me_2Al_2Cl_4$. [d] Procedure. [e] Melting point determined by DSC. [f] Molecular weight and polydispersity determined by GPC/SEC. [g] Total branching determined by ^1H NMR. [h] Results previously reported were based on the nickel loading found by ICP-OES analysis: entry 2: 750; entry 3: 720; entry 4: 530; entry 5: 200; entry 6: 650; entry 7: 280.

loading could result.) Here, we report the ethylene polymerization activities per gram of nickel based on the theoretical *maximum* nickel loading that affords the *minimum* possible activity values. The presumably low ICP-OES analyses (cf. Table 1, entries 2−7) are responsible for the previously reported higher activities per gram of nickel.

Ethylene Polymerization Studies Employing Precatalysts 1b1 and 1b2. The ethylene polymerization activities of precatalysts **1b1** and **1b2** are summarized in Table 1. Slurry polymerizations were performed in 100 mL of pentane under similar conditions (10 mg of **1b1** or **1b2**, 150 psig ethylene). The cocatalyst, ratio of aluminum cocatalyst to nickel precatalyst, nickel loading, polymerization temperature, polymerization time, and polymerization procedure were varied. No PE was obtained when the polymerization was performed in the absence of an alkylaluminum cocatalyst (entry 1), thus attachment of α-diimine nickel(II) complex **11b** to TMA-activated silica support **14a** occurs without a simultaneous activation of precatalyst **1b2**. This feature allows a free choice of the alkylaluminum cocatalyst, and we pursued alternatives less expensive than MAO.

α-Diimine nickel(II) precatalyst **1b1** showed very high productivities when activated with an alkylaluminum halide. Activation with ethylaluminum sesquichloride (EASC) afforded excellent productivities in a 2 h polymerization run at 60 °C.[70] Using **1b1** with a 1.0 wt % nickel loading resulted in

Table 2. Effect of Structural Modifications on the α-Diimine Nickel(II) Precatalysts

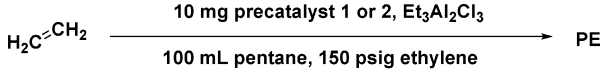

1a: Grace Davison XPO-2402, calcined at 200°C. -MeAl- as linker.
1b1: Grace Davison XPO-2402, calcined at 200°C. -MeAl- as linker.
1c: Grace Davison SP9-496, calcined at 500°C. -MeAl- as linker.
2a1: Grace Davison SP9-496, calcined at 500°C. -MeAl- as linker.
2b: Grace Davison SP9-496, calcined at 500°C. -MeAl- as linker.

entry	precatalyst	*T* [°C]	wt % Ni[a]	time [h]	Al/Ni	proc[b]	kg PE/ g **1/2**	kg PE/ g Ni	T_m [°C][c]	M_w[d] [g/mol]	PDI[d]	branches/ 1000C[e]
1	**1a**	60	1.0	2	280	1b	3.3	330[f]	128	153k	3.6	n.d.
2	**1b1**	60	1.0	2	420	1b	4.5	450[f]	126	131k	3.3	13
3	**1b1**	80	1.0	2	480	1b	1.2	120[f]	122	74k	3.5	n.d.
4	**1c**	60	1.0	1	214	3	1.1	109	120	458k	4.5	54
5	**1c**	60	2.0	1	214	3	1.7	84	118	369k	3.7	54
6	**1c**	80	1.0	1	214	3	0.2	19	119	278k	3.7	64
7	**2a1**	60	1.0	2	214	3	2.0[g]	197	n.d.	596k	15	38
8	**2a1**	80	1.0	2	214	3	0.7[g]	66	n.d.	262k	12	52
9	**2b**	60	1.0	2	214	3	2.1[g]	208	n.d.	825k	18	31
10	**2b**	80	1.0	2	214	3	0.9[g]	96	n.d.	415k	13	48

[a] Theoretical maximum nickel loading. [b] Procedure. [c] Melting point determined by DSC. [d] Molecular weight and polydispersity determined by GPC/SEC. [e] Total branching determined by ^{1}H NMR. [f] Results previously reported were based on the nickel loading found by ICP-OES analysis: entry 1: 580; entry 2: 750; entry 3: 200. [g] A small fraction of oligomers (0.2−0.4 kg per gram of **2a1** or **2b)** was obtained in addition to high-molecular-weight PE with precatalysts **2a1** and **2b**.

productivities of 4.5 kg PE/g **1b1** and 450 kg PE/g of nickel (entry 2). Remarkably, productivities remained high at Al/Ni ratios as low as 48 (430 kg PE/g Ni, entry 3). From these results, it is apparent that EASC is a very efficient activator and that excess EASC does not induce catalyst deactivation. An increase of the nickel loading from 1.0 to 3.0 wt % raised the productivity per gram of **1b1** from 4.5 to 10.8 kg PE without a dramatic loss of the productivity per gram of nickel (entry 4 vs entry 2). Although methylaluminum dichloride (MADC) was found to be less suitable as a cocatalyst at 60 °C (entry 6), the contrary is true when raising the polymerization temperature to 80 °C (entry 7 vs entry 5). Deactivation of homogeneous α-diimine nickel(II) catalysts observed at elevated temperatures of 80 °C is also seen with these supported catalysts.[30] The combination of precatalyst **1b1** with MADC afforded productivities of 1.7 kg PE/g **1b1** and 170 kg PE/g nickel (entry 7). Although absolute activity is lower with MADC as seen at 60 °C, its improved performance at 80 °C compared to EASC is probably attributable to a slower catalyst deactivation.

Initially, 2 h polymerization runs were performed as this is a common residence time in commercial polymerization processes. However, the active species is almost completely deactivated after 1 h, and productivity is only slightly higher after 2 h (entries 8, 9). A common characteristic of these α-diimine nickel(II) catalysts is their extreme activity followed by a rapid decay due to deactivation processes.[18]

Three polymerization procedures were tested in our single-batch reactor (entries 9−11). Productivity and PE properties showed only minor differences upon changes in the procedure. In procedure 3, precatalyst and cocatalyst were added to an argon-filled reactor at room temperature, and the reactor was immediately pressurized with 150 psig ethylene and brought to temperature. This procedure was employed in order to prevent catalyst deactivation in the absence of ethylene. A complication is that some polymerization will take place while heating to the required temperature. Procedures 1a (similar to 1b) and 2 were modified so that the reactor was heated to the polymerization temperature before pressurizing with ethylene. Now polymerization takes place only at the desired temperature, which allows a better comparison with commercial continuous processes. Partial deactivation of the active species during the heating period in the absence of ethylene might explain the slightly reduced productivity of 2.8 kg PE/g **1b2** (entry 10). Saturating the pentane solution prior to heating (procedure 2) showed a small increase in productivity, which suggests that ethylene prevents deactivation (entry 11).

Structural Modifications of the α-Diimine Nickel(II) Precatalysts. Precatalysts **1a**−**c** and **2a,b** were tested in ethylene slurry polymerizations to study the effect of structural modifications (Table 2). Polymerizations were performed in 100 mL of pentane under similar conditions (10 mg of **1a**−**c** or **2a**,**b**, 1 or 2 h, 150 psig ethylene, EASC as cocatalyst, large excess of EASC to nickel precatalyst, polymerization procedure 1b or 3). The polymerization temperature and nickel loading were varied. Entry 3 of Table 1 showed that EASC is a suitable cocatalyst at low Al/Ni ratios; however, in these polymerizations, a larger excess of EASC was used to guarantee a complete activation of the precatalysts. Earlier, we reported that polymerizations with catalysts supported through an amino or hydroxy functionality directly attached to the para position of the aryl α-diimine moiety were disappointing.[67] However, employing a spacer group between these functionalities ($-(CH_2)_3-$ in the case of −OH and $-CH_2(3,5\text{-}CH_3,CH_3-C_6H_2)-$ in the case of $-NH_2$) results in excellent productivities (Table 2). The reasons for the requirement of a spacer are not clear, but it is instructive to note that Herrmann and co-workers observed increasing productivities for silica-attached bis(imino) pyridyl iron ethylene polymerization catalysts with increased length of the carbon chain used for attachment.[65]

Both *ortho*-methyl-substituted α-diimine nickel(II) precatalysts **1a** and **1b1** afforded polyethylenes with quite similar properties (melting point, average molecular weight, polydispersity, and branching). Modifications of the most active precatalyst **1b1** containing *ortho*-methyl groups were pursued in an effort to improve productivity and to influence the polyethylene properties. Introduction of *ortho*-isopropyl substituents was easily achieved and precatalyst **1c** was readily generated, as noted above. Surprisingly, productivities of **1c** relative to **1b1** decreased dramatically at both 60 and 80 °C to 1.1 kg PE/g **1c** and 0.2 kg PE/g **1c**, respectively (entries 4 and 6). Polymerization with precatalyst **1c** having a 2.0 wt % instead of a 1.0 wt % nickel loading (entry 5 vs entry 4) resulted in a

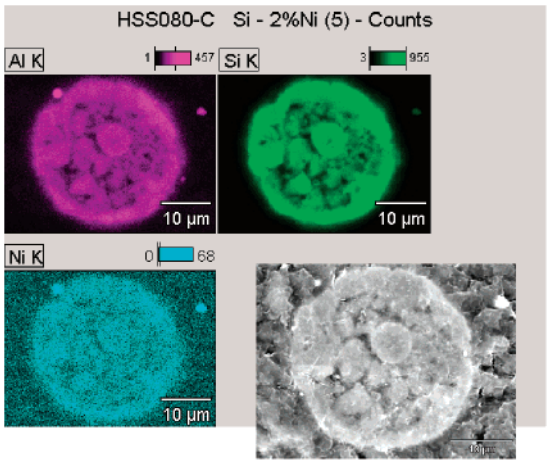

Figure 4. Representive example of a cross-sectioned particle of precatalyst **1c** with a 2.0 wt % nickel loading. EDX mapping of the elements Al−Si−Ni (high brightness reflects high Al−Si−Ni concentrations) and SEM.

similar increase, as was observed when precatalyst **1b1** was supported with a higher nickel loading (Table 1, entry 4). These lower productivities are in sharp contrast to the homogeneous polymerizations.[30] However, interestingly, the polyethylene properties showed a similar trend, as is seen in the homogeneous mode (lower melting temperature, higher average molecular weight, and higher branching level of the isopropyl-substituted system versus the methyl-substituted system). The fact that only the productivity did not follow the "homogeneous" trend stimulated us to investigate this behavior in further detail. These polymerizations are characterized by a high ethylene uptake at the start, which diminishes rapidly compared to the polymerizations with precatalyst **1b1**. One possible explanation of this reduced activity is that the larger α-diimine complex **11c** does not penetrate to the inner surfaces of the mesoporous silica beads. As a consequence, polymer growth would not effectively fragment the silica particle, and an outer coating of PE could develop that would inhibit polymer growth. Energy-dispersive X-ray analysis of cross-sectioned precatalyst particles **1c** with a 2.0 wt % nickel loading was performed to get a better understanding of the distribution of α-diimine complex **11c** (Figure 4). Mapping of Al shows a homogeneous distribution of the trimethylaluminum linker used for the attachment of **11c**. The weight percentage of 2.0 wt % **11c** allowed the successful detection of nickel (mapping of the actual catalytic metal center was not successful in previously reported EDX studies on silica-supported metallocene polymerization catalysts, as its weight percentage was below the detection limit[52,71]), and showed that the hypothesis of a core−shell distribution of **11c** in precatalyst **1c** is incorrect. A homogeneous distribution of nickel was observed within the silica particles after slicing of the beads. SEM of the cross-sectioned particle of precatalyst **1c** showed the locations of the pores within the silica bead, which was also observed by EDX of the elements Al, Si, and Ni (Figure 4).

The physical appearance of the polyethylene particles obtained with precatalyst **1c** were significantly different from those observed with precatalysts **1b1**/**1b2**. The PE particles were analyzed by scanning electron microscopy (SEM), and the resulting micrographs are shown in Figure 5a−c. Figure 5a shows the free-flowing PE particles obtained with precatalyst **1b2** after isolation. Most of these particles are roughly spherical, with a diameter of ∼675 μm. PE particles produced with precatalyst **1c** are somewhat agglomerated after isolation at room temperature; agglomeration intensifies after drying at 70 °C. SEM (Figure 5b) shows these particles are again roughly spherical but smaller in diameter (∼425 μm). The particles appear connected by traces of PE, which are not part of the spherical particles, seemingly consistent with their more aggregated nature.

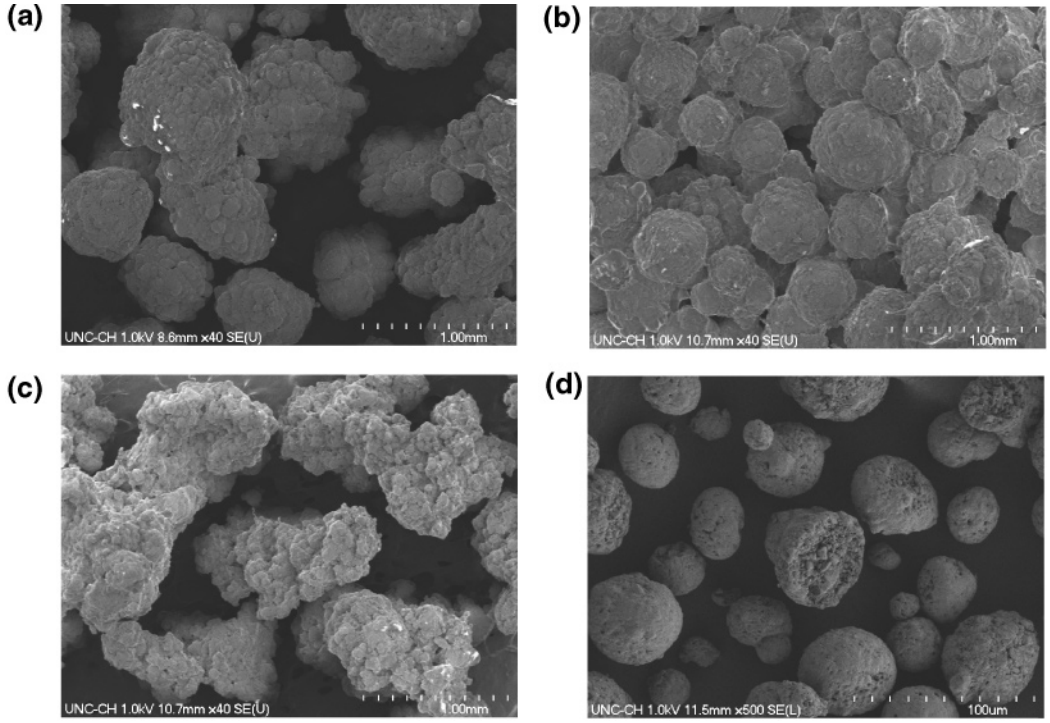

Figure 5. (a) SEM of PE produced in a 1 h polymerization at 60 °C and 150 psig ethylene with precatalyst **1b2** containing a nickel loading of 1.0 wt % (Table 1, entry 8). (b) SEM of PE produced in a 1 h polymerization at 60 °C and 150 psig ethylene with precatalyst **1c** containing a nickel loading of 1.0 wt % (Table 2, entry 4). (c) SEM of PE produced in a 2 h polymerization at 80 °C and 700 psig ethylene with precatalyst **1b2** containing a nickel loading of 1.0 wt % (Table 6, entry 7). (d) SEM of Grace Davison SP9-496 that is calcined at 500 °C.

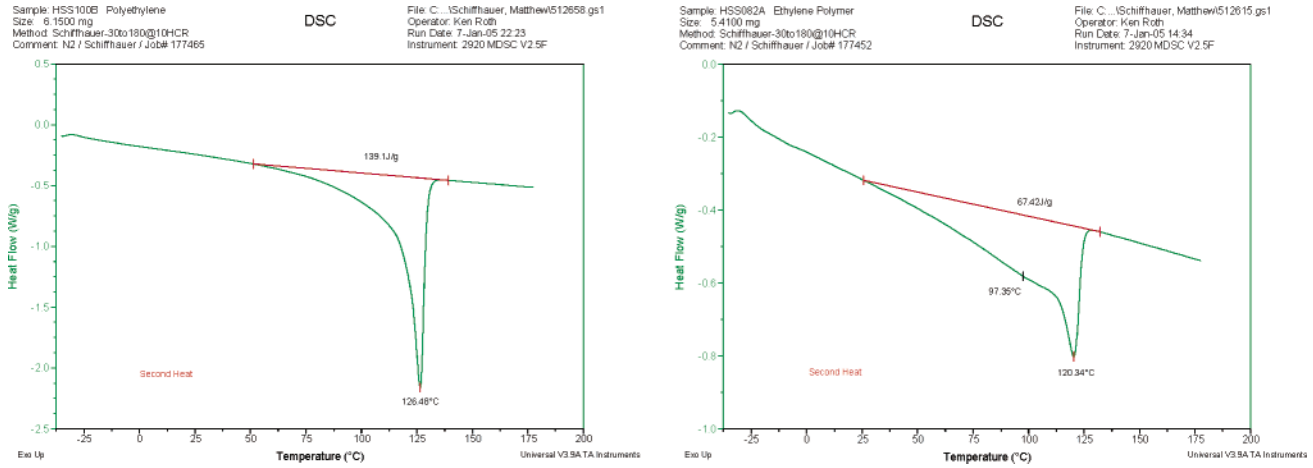

Figure 6. (a) DSC of PE produced in a 1 h polmerization at 60 °C and 150 psig ethylene with precatalyst **1b2** containing a nickel loading of 1.0 wt % (Table 1, entry 8). (b) DSC of PE produced in a 1 h polymerization at 60 °C and 150 psig ethylene with precatalyst **1c** containing a nickel loading of 1.0 wt % (Table 2, entry 4).

Table 3. ^{13}C NMR Analysis of PE Produced in a 1 h Polymerization at 60 °C and 150 psig Ethylene with Precatalysts 1b2 (Table 1, Entry 8) and 1c (Table 2, Entry 4) Containing a Nickel Loading of 1.0 wt %[43]

	branches per 1000 CH_2								
precatalyst	methyl	ethyl	propyl	butyl	amyl	butyl+, EOC	amyl+, EOC	hexyl+, EOC	total branches
1b2	13.5	1.9	0.6	0.6	0.3	1.5	0.7	0.9	17.6
1c	36.8	4.1	1.9	1.2	1.0	4.5	3.0	1.7	47.4

Branching densities and types of branches for the PE's produced with the precatalysts **1b2** and **1c** were determined by ^{13}C NMR spectroscopy (Table 3). The branching densities measured by ^{13}C NMR agree with those determined by ^{1}H NMR and show ca. 20 branches/1000Cs for PE from **1b2** and ca. 50 branches/1000Cs for PE from **1c**. Differential scanning calorimetry (DSC) analysis showed interesting features for these PE's (Figure 6). PE from **1b2** with 20 branches/1000Cs shows a fairly broad endotherm with a T_m of 126 °C (Figure 6a) and is typical of solution-generated PE containing a similar number of branches.[30] The PE from **1c** exhibits an extremely broad endotherm, but a clear, prominent T_m at 120 °C (Figure 6b). On the basis of solution results, a PE containing 50 branches/1000Cs would be expected to exhibit a much lower T_m than the observed 120 °C.[30] A plausible explanation is that the branches are not evenly distributed along these chains. This could result if the nickel active centers become increasingly buried in growing polymer and the effective ethylene concentration at these centers is reduced. On the basis of previous results,[18,30] lower effective concentrations of ethylene give rise to increased branching, indicating that these polymers may be tapered with the more linear segments, giving rise to the prominent T_m at 120 °C. The more amorphous segments may be responsible for agglomeration of these particles.

^{13}C NMR analysis afforded more detailed information compared to ^{1}H NMR analysis, which only provides the total number of branches.[43,44] The ^{13}C NMR analysis allowed us to clarify the nature of the branches and the amount of each branch in the PE chains (Table 3). Both PE's obtained with precatalysts **1b2** and **1c** contain the same types of branches in approximately the same ratios, with the amount of each branch decreasing from short to long chains. This is a consequence of the chain-walking mechanism involved in the enchainment process, as has been earlier documented[18,29] and summarized above.

Covalent attachment in the aryl α-diimine nickel(II) precatalysts **2a1** and **2b** was achieved using either one or two hydroxy-tails in the backbone. These catalysts are more closely related to the diimine catalysts containing methyl groups in the backbone rather than those containing the acenaphthyl group in the backbone (see Figure 1). Productivities were significantly lower (ca. 2×) compared to those observed with precatalyst **1b1** at both 60 and 80 °C (Table 2, entries 7−10). Productivities and PE properties of PEs obtained with **2a1** and **2b** are similar, which suggests that a second hydroxyl functionality has no effect on the performance of the catalyst. The increase in average molecular weight for these precatalysts **2** with an alkyl-substituted backbone compared to precatalysts **1** with a planar aromatic acenaphthyl backbone is also observed with the unsupported catalysts.[29,30] The molecular weight distributions of PE from precatalysts **2** are very broad compared to PE from precatalysts **1**.

Polymerizations with precatalysts **1b** produced exclusively high-molecular-weight PE particles; no formation of fines and indications of catalyst leaching were observed nor was there any reactor fouling. In the case of precatalyst **1c**, while mainly free-flowing PE particles were obtained, a small amount of PE did adhere to the reactor wall and stirring blade. This seems likely due to the low melting properties and more amorphous nature of the PE.

In general, the same changes in the PE properties were observed for precatalysts **1** and **2** upon increased polymerization temperatures. Higher temperatures resulted in a decrease of the average molecular weight together with a decrease of the melting point due to increased branching densities. The same behavior had been observed for the unsupported catalysts.[30] However, clear differences are observed for the polymer properties when produced with supported or unsupported catalysts. Average molecular weight, polydispersity, and melting point are in general higher and branching densities lower for the supported catalysts under similar conditions. These features have also been observed for polymerizations using α-diimine nickel(II) catalysts supported with other technologies.[54,55] Reduced branching suggests a reduced propensity for chain walking in supported catalysts.

Silica Support: Effect of Calcining Temperatures. α-Diimine nickel(II) complex **12a** was supported on three different

Table 4. Influence of the Calcining Temperature of the Silica Support[a]

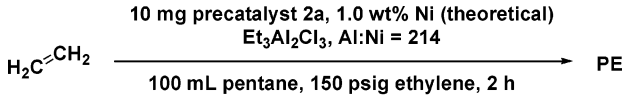

2a1: Grace Davison SP9-496, calcined at 500°C. -MeAl- as linker.
2a2: Grace Davison SP9-496, calcined at 600°C. -MeAl- as linker.
2a3: Grace Davison SP9-496, calcined at 700°C. -MeAl- as linker.

entry	precatalyst	silica **13** [mmol OH/g]	*T* [°C]	kg PE/g **2a**	kg PE/g Ni
1	**2a1**	1.36	60	2.0[b]	197
2	**2a1**	1.36	80	0.7[b]	66
3	**2a2**	1.25	60	1.5[b]	151
4	**2a2**	1.25	80	0.7[b]	66
5	**2a3**	1.07	60	1.8[b]	184
6	**2a3**	1.07	80	0.7[b]	66

[a] Procedure. [b] 0.2 to 0.4 kg oligomers per gram of precatalyst 2a isolated for each polymerization.

activated silica supports **14a**. The Grace Davison SP9-496 silicas used for the preparation of **14a** were calcined at different temperatures of 500, 600, and 700 °C. Calcination allows control of the number of free hydroxy functionalities on silica **13**,[52] which decreases with an increasing calcination temperature from 1.36 mmol OH/g **13** at 500 °C to 1.25 at 600 °C to 1.07 at 700 °C. Slurry polymerizations with precatalysts **2a1**, **2a2**, and **2a3** were performed to study the effect of the calcination temperature (Table 4). Polymerization runs of 2 h were performed under the same conditions (10 mg of **2a**, 1.0 wt % Ni, EASC, Al/Ni = 214) in 100 mL of pentane at 150 psig ethylene. Similar productivities of around 1.8 kg PE/g **2a** were obtained at 60 °C (compare entries 1, 3, 5), and the same productivities of 0.7 kg PE/g **2a** were observed at 80 °C (compare entries 2, 4, 6). Apparently, 1.07 mmol of TMA-linked hydroxy functionalities is sufficient to quantitatively support a 1.0 wt % nickel loading of α-diimine nickel(II) complex **12a**, and the presence of additional $SiOAlMe_2$ functionalities on precatalysts **2a1** and **2a2** do not effect the polymerization.

Silica-Support Linker. Grace Davison SP9-496 silica was treated with the linkers trimethylaluminum, tetrachlorosilane, and trichloroborane. Covalent attachment of α-diimine nickel(II) complex **11b** to the linker of the silica supports **14a** (−$AlMe_2$), **14b** (−$SiCl_3$), and **14c** (−BCl_2) afforded precatalysts **1b2**, **1b3**, and **1b4**, respectively. The effect of the support linker was tested under the same polymerization conditions (10 mg of **1b**, 1.0 wt % Ni, EASC, Al/Ni = 214, 2 h) in 100 mL of pentane at 150 psig ethylene (Table 5). Trimethylaluminum (entries 1−2) was found to be an excellent linker in our initial studies. Methane is released in both the attachment of the linker to the silica support and upon attachment of α-diimine nickel(II) complex **11b** (Scheme 6). The TMA-treated silica support **14a** does not activate complex **11a** in the grafting reaction. In an attempt to find a less-expensive alternative to TMA, we screened tetrachlorosilane and trichloroborane as linkers. These linkers have in common that HCl is released upon attachment to the support and attachment of complex **11b**. Similar productivities were obtained with the −$SiCl_2$− (**1b3**) and −BCl− (**1b4**) precatalysts at 60 and 80 °C (compare entries 3, 5 to 4, 6). The somewhat lower productivities obtained at 60 °C (entries 3 and 5) compared with that obtained with TMA precatalyst **1b2** (entry 1) might be ascribed to an incomplete removal of HCl. However, all three precatalysts afforded similar productivities at 80 °C (compare entries 2, 4, 6).

Effects of Variation of Ethylene Pressure. An ethylene pressure of 150 psig was chosen as the standard pressure for

Table 5. Influence of the Silica Support Linker[a]

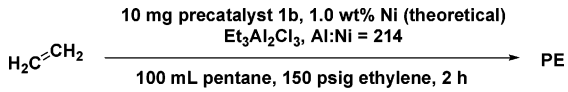

1b2: Grace Davison SP9-496, calcined at 500°C. -MeAl- as linker.
1b3: Grace Davison SP9-496, calcined at 500°C. -Cl_2Si- as linker.
1b4: Grace Davison SP9-496, calcined at 500°C. -ClB- as linker.

entry	precatalyst	linker	*T* [°C]	kg PE/g **1b**	kg PE/g Ni
1	**1b2**	Me_3Al	60	3.6	355
2	**1b2**	Me_3Al	80	1.3	130
3	**1b3**	$SiCl_4$	60	2.7	268
4	**1b3**	$SiCl_4$	80	1.1	114
5	**1b4**	BCl_3	60	2.8	277
6	**1b4**	BCl_3	80	1.2	117

[a] Procedure 3.

screening and evaluation of catalysts. However, because commercial slurry polymerizations are generally operated at higher ethylene pressures (400−700 psig), we have examined these systems in this pressure range. Slurry polymerizations were performed using precatalysts **1b2** and **1c** under similar conditions (See Table 6: 10 mg of **1b2** or **1c**, 1.0 wt % Ni, EASC, Al/Ni = 214, 2 h, 100 mL of pentane). Polymerization using **1b2** at 75 psig ethylene showed a productivity of 2.0 kg PE/g **1b2** at 60 °C (entry 1). Increasing ethylene pressure to 150 to 400 to 700 psig resulted in improved productivities of 2.8 to 4.4 to 4.8 kg PE/g **1b2**, respectively (entries 2−4). This effect of ethylene pressure was previously observed for homogeneous α-diimine nickel(II) catalysts.[30,72] Qualitative monitoring of ethylene uptake suggests that catalyst lifetimes are somewhat increased at higher ethylene pressures. A major challenge with α-diimine nickel(II) catalysts is to achieve high productivities at 80 °C, a temperature appropriate for commercial slurry processes. Increased ethylene pressures in part address this problem. The productivity of **1b2** at 80 °C was doubled when the pressure was increased from 150 to 700 psig ethylene (entry 5 vs entry 7). Surprisingly, polymerization with *ortho*-isopropyl-substituted precatalyst **1c** at 700 psig ethylene (entry 8) showed an excellent productivity of 2.2 kg PE/g **1c**. This is a 10-fold increase compared to the polymerization at 150 psig (Table 2, entry 6). Furthermore, productivity is now comparable to that of precatalyst **1b2** (2.7 kg PE/g precatalyst), which is in sharp contrast to what was seen at 150 psig.

Free flowing PE particles were obtained in all polymerization runs with precatalyst **1b2**. The spherical morphology of Grace Davison SP9-496 silica particles (Figure 5d) is reproduced in the PE particles at 150 psig ethylene and 60 °C (Figure 5a).[10,71,73,74] However, the morphology of the PE particles produced at 700 psig ethylene and 80 °C (Figure 5c) is somewhat different from that obtained at 150 psig ethylene. Particle diameters are greater (compare Figure 5a and c), but their somewhat irregular shapes suggest some particle fragmentation during growth.

A clear trend was seen for the PE properties with an increasing ethylene pressure. Melting temperature and average molecular weight increased steadily going from 75 to 150 to 400 psig ethylene at both 60 and 80 °C. This trend was also observed for the unsupported catalysts.[30] However, this trend was reversed in going from 400 to 700 psig as melting point and average molecular weight decreased. This might indicate that, at 700 psig, the local temperature in the growing PE particles exceeds 80 °C and thus increases branching and decreases T_m. Consistent with polymerizations in homogeneous solutions,[30] the isopropyl-substituted system **1c** relative to **1b2**

Table 6. Influence of the Ethylene Pressure[a]

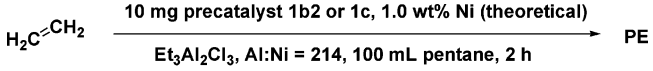

1b2: Grace Davison SP9-496, calcined at 500°C, -MeAl- as linker.
1c: Grace Davison SP9-496, calcined at 500°C, -MeAl- as linker.

entry	precatalyst	pressure [psig]	T [°C]	kg PE/g **1b2**/**1c**	kg PE/g Ni	T_m[b] [°C]	M_w[c] [g/mol]	PDI[c]
1	**1b2**	75	60	2.0	200	124	121k	6.2
2	**1b2**	150	50	2.8	280	126	149k	8.2
3	**1b2**	400	60	4.4	440	130	166k	7.2
4	**1b2**	700	60	4.8	483	126	127k	5.1
5	**1b2**	150	80	1.4	136	122	76k	5.0
6	**1b2**	400	80	2.1	211	128	119k	7.6
7	**1b2**	700	80	2.7	272	127	105k	4.5
8	**1c**	700	80	2.2	219	117	338k	4.2

[a] Procedure 1a. [b] Melting point determined by DSC. [c] Molecular weight and polydispersity determined by GPC/SEC.

Table 7. Influence of the Nickel Loading[a]

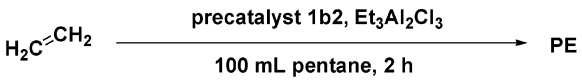

1b2: Grace Davison SP9-496, calcined at 500°C, -MeAl- as linker.

entry	precatalyst [mg]	wt% Ni[b]	Al/Ni	pressure [psig]	T [°C]	kgPE/g **1b2**	kg PE/g Ni	T_m [°C][c]	M_w[d] [g/mol]	PDI[d]
1	10.0	1.0	214	400	80	2.1	211	128	119k	7.6
2	10.0	1.0	214	700	80	2.7	272	127	105k	4.5
3	10.0	3.0	143	400	80	1.9	63	123	61k	4.3
4	5.0	3.0	143	400	80	4.9	164	124	90k	4.6
5	5.0	3.0	143	700	80	6.0	200	125	94k	4.8
6	5.0	3.0	143	700	90	3.9	130	125	78k	4.3

[a] Procedure 1a. [b] Theoretical maximum nickel loading. [c] Melting point determined by DSC. [d] Molecular weight and polydispersity determined by GPC/SEC.

under similar conditions yields PE with increased molecular weight and decreased melting temperature.

Variation of Nickel Loadings. Polymerization runs at 60 °C and 150 psig ethylene with precatalyst **1b1** showed an increased productivity per gram of **1b1** of 4.5 to 10.8 kg PE by increasing the Ni loading from 1.0 to 3.0 wt % (Table 1, entries 2 and 4). Considering the increase in productivity with increasing ethylene pressure, we screened **1b2** with 3.0 wt % Ni loading at pressures of 400 and 700 psig. Slurry polymerizations were performed under similar conditions (EASC, Al/Ni = 143, 2 h) in 100 mL of pentane at 80 or 90 °C (Table 7). Polymerization at 400 psig ethylene with 10 mg of precatalyst resulted in a rapid temperature increase in the autoclave from 80 to 115 °C as the cooling capacity was unable to control this extreme exotherm. The PE produced was agglomerated, and the loss of particle morphology suggests that the actual temperature in the particles passed 115 °C. This exotherm no doubt deactivated the catalyst and accounts for the lowered productivity relative to the run using a 1.0 wt % Ni loading. When the precatalyst loading was reduced from 10 to 5 mg, the temperature could be controlled and maintained at ca. 80 °C (a slight exotherm to 86 °C was initially observed, entry 4). Now, productivity per gram of **1b2** at 400 psig increased from 2.1 kg PE/g **1b2** (150psig) to 4.9 kg PE/g **1b2** with little loss of productivity on a per-gram Ni basis. The best productivity at 80 °C was 6.0 kg PE/g **1b2** obtained at 700 psig ethylene (entry 5). The value of 6.0 kg PE/g support at 80 °C conforms to requirements for applications in commercial slurry reactors.[75] Although reduced, polymerization at 90 °C, 3.0 wt % Ni loading showed a surprisingly good productivity of 3.9 kg PE/g **1b2** (entry 6).

These polymerization conditions not only affect productivity but also the PE properties. Melting points and average molecular weights were significantly lower when precatalyst **1b2** was supported with a 3.0 wt % nickel loading instead of 1.0 wt % (entries 3−6 vs 1−2). It seems likely that this is due to the large exotherm and heating of the particles above the solution temperature. This proposal is strengthened by the observed melting point of 123 °C and average molecular weight of 61k in run 3, during which the solution temperature rose to 115 °C.

Conclusion

α-Diimine nickel(II) catalysts covalently linked to silica supports are highly productive ethylene homopolymerization catalysts. α-Diimine ligands with pendant amino and hydroxy functionalities are easily prepared via standard synthetic procedures, and formation of the nickel(II) complexes was achieved without the use of protecting groups. Reaction of these functionalities with the linker of a silica support resulted in the desired covalent attachment of the nickel(II) complexes. Trimethylaluminum, tetrachlorosilane, and trichloroborane were identified as efficient linkers, with trimethylaluminum as the preferred one. This approach enabled high catalyst loadings, and activation of these supported precatalysts with alkylaluminum cocatalysts afforded highly productive ethylene polymerization catalysts.

Development of this technology in slurry polymerizations demonstrated the following: (1) Inexpensive ethylaluminum sesquichloride is a very efficient cocatalyst even at low Al/Ni ratios. (2) Polyethylene properties, including melting points, molecular weights, and branching densities, can be varied by modification of the *ortho*-aryl substituents. (3) Ethylene pressure is a crucial parameter for optimization of productivity. Productivity increases steadily as ethylene pressure is raised from 150 to 700 psig, and at 700 psig, high productivities can be achieved at temperatures up to 80 °C. (4) An increase in nickel loading from 1.0 to 3.0 wt % results in a significant increase in

productivity on a kg PE/g heterogeneous catalyst basis with only minor decreases in productivity on a kg PE/g Ni basis. Using a 3.0 wt % Ni loading in combination with an ethylene pressure of 700 psig, productivities of up to 6.0 kg PE/g precatalyst at 80 °C can be obtained. (5) No reactor fouling due to leaching of the catalyst is observed.

These observations demonstrate productivities and temperature and pressure ranges compatible with many commercial slurry reactors used for PE production and suggest possible utility of these supported nickel α-diimine catalysts in such reactors.

Experimental Section

General Methods. All reactions involving oxygen- and/or water-sensitive compounds were carried out under an argon atmosphere in dried glassware using standard Schlenk, syringe, and septa techniques. Argon was purified by passage through columns of BASF R3−11 catalyst (Chemalog) and 4 Å molecular sieves. Oxygen- and/or water-sensitive compounds were transferred or manipulated in an argon-filled glovebox at room temperature. Thin-layer chromatography was carried out on Whatman silica, 250 μm layer, flexible plates for TLC, PE, SIL, G/UV. Flash chromatography was performed using Scientific Adsorbents silica gel no. 02826-25, particle size 22−63 μm, pore size 60 Å.[76] ^{1}H and ^{13}C NMR spectra were recorded on a Bruker Avance 300 MHz spectrometer in $CDCl_3$ or CD_2Cl_2. Chemical shifts are reported relative to residual $CHCl_3$ (δ 7.26 for ^{1}H), residual $CHDCl_2$ (δ 5.32 for ^{1}H), $CDCl_3$ (δ 77.00 for ^{13}C), and CD_2Cl_2 (δ 53.7 for ^{13}C). Chemical shifts δ are quoted in parts per million (ppm), and coupling constants J are given in hertz (Hz). Mass spectra were recorded on a Micromass Quattro II triple quadrupole mass spectrometer in ESI mode. Elemental analyses was performed by Atlantic Microlab of Norcross, GA. X-ray diffraction data were collected on a Bruker SMART 1K diffractometer using the Ω scan mode (see Supporting Information for crystallographic information file). High-temperature gel permeation chromatography (GPC/SEC) was performed by DuPont (Wilmington, DE) in 1,2,4-trichlorobenzene at 135 °C using a Waters GPCV2000-TCB dual/triple detector instrument. A calibration curve was established with polystyrene standards and universal calibration was applied using Mark−Houwink constants for polyethylene ($k = 4.34 \times 10^{-4}$; $\alpha = 0.724$). Differential scanning calorimetry (DSC) data were recorded on a Seiko Instruments DSC 220. Melting points were recorded in the second heating run at a heating rate of 10 °C/min. ^{1}H NMR spectra of polyethylenes were recorded in C_6D_5Br at 120 °C. The formula used to calculate branching was $(CH_3/3)/[CH + (CH_2/2) + (CH_3/3)] \times 1000$ = branches per 1000 carbons. CH_3, CH_2, and CH refer to the integration obtained for the methyl, methylene, and methine resonances, respectively. High-molecular-weight polyethylene was obtained in all instances, which made correction for methyl end groups unnecessary.[77] ^{13}C NMR spectra of polyethylenes were recorded in a 0.05 M $Cr(acac)_3$ solution in C_6D_5Br with 15 wt % polyethylene. Signals were assigned as described by Cotts.[43] Nickel contents of silica-supported nickel diimine precatalysts and the residual nickel contents of the dichloromethane solutions used for the support reaction were determined with inductively coupled plasma spectrometry (ICP-OES) and were performed by DuPont (Wilmington, DE). Scanning electron microscopy (SEM) of silica and PEs was performed on a Hitachi S-4700 scanning electron microscope. Scanning electron microscopy (SEM) of cross-sectioned particles of silica-supported nickel diimine precatalysts and the distribution of the elements Al−Si−Ni in these particles was determined on a scanning electron microscope (SEM) equipped with an energy-dispersive X-ray spectrometer (EDX), and was performed by DuPont (Wilmington, DE). Precatalyst particles were embedded in low-viscosity epoxy resin and cut with a razor blade after cooling the sample in liquid nitrogen in order to obtain the cross-sectioned particles. Charging of the cross-sectioned particles was prevented by an additional carbon coating.

Materials. Polymer-grade ethylene (99.5%) and hydrogen were purchased from National Speciality Gases. Ethylene was purified over a 30% Cu/SiO_2 catalyst and molecular sieves, and hydrogen was used without purification. $Et_3Al_2Cl_3$ (0.91 M in toluene), Me_3-Al (2 M in hexane), palladium acetate, tri-*o*-tolyl phosphine, anhydrous triethylamine, methyl acrylate, lithium aluminum hydride, 10% palladium on activated carbon, $NiBr_2$(1,2-dimethoxyethane), bromine, diisopropylamine, *n*-butyllithium (1.6 M in hexane), tetrabutylammoniumfluoride (1 M in THF), sodium iodide, chlorotrimethylsilane, tetrachlorosilane, trichloroborane, *p*-toluenesulfonic acid, **3**, **5**, **6a**, and **7** were used as purchased from Aldrich Chemical Co. $CDCl_3$, CD_2Cl_2, and C_6D_5Br were purchased from Cambridge Isotope Laboratories. Grace Davison silicas were used as received. The compounds **1a**,[67] **1b1**,[67] **6b**,[67] **8a**−**b**,[67] **9**,[78] **11a**−**b**,[67] **14a**,[67] and (6-iodo-hexyloxy)-trimethyl-silane[79,80] were prepared according to literature procedures. Toluene, dichloromethane, diethyl ether, and pentane were passed through an activated alumina column.[81] Tetrahydrofuran was freshly distilled from sodium/benzophenone.

3-(4-Amino-3,5-diisopropyl-phenyl)-propan-1-ol (6c). A modified literature procedure was used for the synthesis of **4**, and the spectral data were in agreement with those previously reported.[82] Aniline **3** (35.0 g, 197 mmol, 1.00 equiv), bromine (11.2 mL, 217 mmol, 1.10 equiv), and 350 mL of acetic acid were used. Column chromatography (flash silica, eluent; ethyl acetate/hexane = 1:19) afforded **4** in 35% yield (17.5 g, 68.2 mmol). The procedure reported previously for the synthesis of **6b** was used for the synthesis of **6c** from **4**.[67] Palladium acetate (138 mg, 0.60 mmol, 0.01 equiv), tri-*o*-tolyl phosphine (1.50 g, 4.90 mmol, 0.08 equiv), and 60 mL of toluene were mixed under an argon atmosphere. Anhydrous triethylamine (24.6 mL, 176 mmol, 2.87 equiv), **4** (15.7 g, 61.4 mmol, 1.00 equiv), and methyl acrylate (6.9 mL, 76.1 mmol, 1.24 equiv) were added in this order at 20 °C. The reaction mixture was heated to 100 °C and stirred for 6 h at this temperature, after which it was added to water. The water layer was extracted three times with diethyl ether, and the organic layer was dried over $MgSO_4$. Removal of the solvent in vacuo resulted in the isolation of the crude 3-(4-amino-3,5-diisopropyl-phenyl)-acrylic acid methyl ester (20.6 g), which was used without further purification. This mixture (20.6 g) was dissolved in 400 mL of THF, and lithium aluminum hydride (5.97 g, 157 mol) was added at 0 °C. The temperature was raised to 20 °C after complete addition, and the reaction mixture was stirred for 30 min at this temperature. The reaction mixture was poured into water. The water layer was extracted with diethyl ether, and the collected organic fractions were dried over $MgSO_4$. The solvent was removed in vacuo. Column chromatography (flash silica, eluent; ethyl acetate/hexane = 1:2) afforded a mixture of 3-(4-amino-3,5-diisopropyl-phenyl)-prop-2-en-1-ol and **6c** (8.41 g). The mixture was dissolved in 100 mL of ethyl acetate, and palladium (10 wt %) on activated carbon (100 mg, 0.09 mmol) was added. Hydrogen was slowly purged through the solution for 16 h at 20 °C. Removal of the palladium catalyst and the solvent resulted in the isolation of **6c** as a brown oil (7.67 g, 32.6 mmol). Aniline **6c** was synthesized in an overall yield of 18% based on **3**. $R_f = 0.59$ (ethyl acetate/hexane = 1:1); ^{1}H NMR (300.1 MHz, CD_2Cl_2, 298 K) δ: 6.84 (s, 2H), 3.70−3.54 (m, 4H), 2.91 (septet, $J = 6.9$, 2H), 2.56 (t, $J = 7.8$, 2H), 1.81 (tt, $J = 7.8$, $J = 6.6$, 2H), 1.31 (bs, 1H), 1.24 (d, $J = 6.9$, 12H).

3-{4-[2-[4-(3-Hydroxy-propyl)-2,6-diisopropyl-phenylimino]-2H-acenaphthylen-1-ylideneamino]-3,5-diisopropyl-phenyl}-propan-1-ol (8c). A procedure reported previously in the literature was used for the synthesis of **8c**.[67] Acenaphthenequinone (516 mg, 2.83 mmol, 1.00 equiv), **6c** (2.00 g, 8.50 mmol, 3.00 equiv), and concentrated aqueous H_2SO_4 (0.10 mL) were added to 60 mL of toluene. This mixture was refluxed for 16 h. Column chromatography (flash silica, eluent; ethyl acetate/hexane = 1:1) afforded α-diimine **8c** as a yellow solid in 48% yield (828 mg, 1.34 mmol). $R_f = 0.24$ (ethyl acetate/hexane = 1:1); ^{1}H NMR (300.1 MHz, CD_2Cl_2, 298 K) δ: 7.89 (d, $J = 7.8$, 2H), 7.36 (dd, $J = 7.8$, $J = 7.8$, 2H), 7.12 (s, 4H), 6.66 (d, $J = 7.8$, 2H), 3.75 (dt, $J = 7.7$, $J = 6.2$, 4H), 2.94 (septet, $J = 6.9$, 4H), 2.78 (t, $J = 7.7$, 4H), 1.98 (m,

4H), 1.41 (bs, 2H), 1.20 (d, $J = 6.9$, 12H), 0.98 (d, $J = 6.9$, 12H); $^{13}C\{^1H\}$ NMR (100.6 MHz, CD_2Cl_2, 298 K) δ: 161.3 (C═N), 145.9 (q C), 141.1 (q C), 138.1 (q C), 135.4 (q C), 131.5 (q C), 130.0 (q C), 129.1 (CH), 128.2 (CH), 123.9 (CH), 123.4 (CH), 62.8 (CH_2), 35.3 (CH_2), 32.6 (CH_2), 29.0 (CH), 23.2 (CH_3), 23.1 (CH_3); MS-ESI *m*/*z* (%): $C_{42}H_{53}N_2O_2$ $[M + H]^+$ 617.0 (100%). Anal. Calcd for $C_{42}H_{52}N_2O_2$: C, 81.78; H, 8.50; N, 4.54. Found: C, 81.73; H, 8.50; N, 4.56.

8,9-Bis-[(E)-2,6-dimethyl-phenylimino]-decan-1-ol (10a). A procedure reported previously in the literature was used for the synthesis of **10a**.[83] α-Diimine **9** (4.0 g, 13.7 mmol, 1.00 equiv) was dissolved in THF, and a THF solution of LDA (13.7 mmol, 1.00 equiv, prepared from diisopropylamine (2.20 mL, 15.7 mmol, 1.15 equiv) and *n*-butyllithium (8.55 mL, 13.7 mmol, 1.00 equiv, 1.6 M solution in hexane) was added at −50 °C. The color of the reaction mixture turned from yellow to red. The reaction mixture was slowly brought to 20 °C and stirred for an additional hour at this temperature. The reaction mixture was cooled to −50 °C, and (6-iodo-hexyloxy)-trimethylsilane (4.11 g, 13.7 mmol, 1.00 equiv) was added at once. The reaction mixture was stirred for 16 h at 20 °C. The reaction was completed when the color turned from black to bright yellow. Tetrabutylammoniumfluoride (14.0 mL, 14.0 mmol, 1.02 equiv, 1 M solution in THF) was added. The solvent was removed in vacuo, and the isolated oily material was purified by column chromatography (flash silica, ethyl acetate/hexane = 1:1). α-Diimine **10a** was isolated as a bright-yellow oil in a 82% yield (4.54 g). ^1H NMR (300.1 MHz, $CDCl_3$, 298 K) δ: 7.03 (m, 4H), 6.91 (m, 2H), 3.54 (m, 2H), 2.47 (m, 2H), 2.02 (s, 12H), 2.00 (s, 3H), 1.44 (m, 4H), 1.23 (m, 6H); $^{13}C\{^1H\}$ NMR (75.4 MHz, $CDCl_3$, 298 K) δ: 171.5, 167.5, 148.4, 147.9, 127.9, 124.6, 124.5, 123.1, 62.6, 53.7, 32.5, 29.7, 29.0, 28.8, 26.5, 25.3, 18.0, 17.9. Anal. Calcd for $C_{26}H_{36}N_2O$: C, 79.55; H, 9.24; N, 7.14. Found: C, 79.17; H, 9.56; N, 7.14.

8,9-Bis-[(*E*)-2,6-dimethyl-phenylimino]-hexadecane-1,16-diol (10b). The same procedure was used as for **10a**.[83] The only difference was that the second substitution was performed before deprotection with tetrabutylammoniumfluoride: first substitution: α-diimine **9** (3.00 g, 10.3 mmol, 1.00 equiv), (6-iodohexyloxy)-trimethylsilane (3.08 g, 10.3 mmol, 1.00 equiv), diisopropylamine (1.44 mL, 10.3 mmol), and *n*-butyllithium (6.41 mL, 10.3 mmol, 1.6 M solution in hexane); second substitution: (6-iodohexyloxy)-trimethylsilane (3.08 g, 10.3 mmol, 1.00 equiv), diisopropylamine (1.44 mL, 10.3 mmol), *n*-butyllithium (6.41 mL, 10.3 mmol, 1.6 M solution in hexane), and tetrabutylammoniumfluoride (20.6 mL, 20.6 mmol, 2.00 equiv, 1 M solution in THF). The solvent was removed in vacuo, and the isolated oily material was purified by column chromatography (flash silica, ethyl acetate). α-Diimine **10b** was isolated as a bright-yellow oil in a 65% yield (3.31 g). ^1H NMR (300.1 MHz, $CDCl_3$, 298 K) δ: 7.05 (m, 2H), 6.93 (m, 1H), 3.54 (m, 2H), 2.46 (m, 2H), 2.03 (s, 6H), 2.01 (s, 3H), 1.44 (m, 4H), 1.23 (m, 6H); $^{13}C\{^1H\}$ NMR (75.4 MHz, $CDCl_3$, 298 K) δ: 171.1, 148.0, 127.9, 124.7, 123.0, 62.7, 32.5, 29.7, 29.2, 28.8, 26.3, 25.3, 18.1; Anal. Calcd for $C_{32}H_{48}N_2O_2$: C, 78.00; H, 9.82; N, 5.69. Found: C, 77.75; H, 9.85; N, 5.66.

3-{4-[2-[4-(3-Hydroxypropyl)-2,6-diisopropyl-phenylimino]-2H-acenaphthylen-1-ylideneamino]-3,5-diisopropyl-phenyl}-propan-1-ol Nickel Dibromide (11c). A procedure reported previously in the literature was used for the synthesis of **11c**.[30,67] α-Diimine **8c** (250 mg, 0.41 mmol, 1.05 equiv) and $NiBr_2$(dme) (119 mg, 0.39 mmol, 1.00 equiv) were suspended in 10 mL of dichloromethane. The reaction mixture was stirred for 16 h at 20 °C. The dichloromethane was removed in vacuo at 20 °C, and the residual solids were washed with diethyl ether (3 × 5 mL). $NiBr_2$ complex **11c** was isolated as a brown solid in a 83% yield (270 mg, 0.32 mmol). Anal. Calcd for $C_{42}H_{52}Br_2N_2NiO_2$: C, 60.39; H, 6.27; N, 3.35. Found: C, 58.54; H, 6.18; N, 3.17.

8,9-Bis-[(*E*)-2,6-dimethyl-phenylimino]-decan-1-ol Nickel Dibromide (12a). The same procedure was used as for **11c**.[30,67] α-Diimine **10a** (1.00 g, 2.54 mmol, 1.00 equiv), $NiBr_2$ (dme) (780 mg, 2.54 mmol, 1.00 equiv), and 60 mL of dichloromethane were used. $NiBr_2$ complex **12a** was isolated as a brown solid in a 86% yield (1.34 g, 2.18 mmol). Crystals suitable for X-ray analysis were obtained by a slow diffusion crystallization of pentane into a saturated dichloromethane solution. Anal. Calcd for $C_{26}H_{36}Br_2N_2NiO$: C, 51.10; H, 5.94; N, 4.58. Found: C, 51.80; H, 6.29; N, 4.54.

8,9-Bis-[(*E*)-2,6-dimethyl-phenylimino]-hexadecane-1,16-diol Nickel Dibromide (12b). The same procedure was used as for **11c**.[30,67] α-Diimine **10b** (1.18 g, 2.39 mmol, 1.00 equiv), $NiBr_2$(dme) (730 mg, 2.39 mmol, 1.00 equiv), and 60 mL of dichloromethane were used. $NiBr_2$ complex **12b** was isolated as a brown solid in a 51% yield (0.87 g, 1.22 mmol). Anal. Calcd for $C_{32}H_{48}Br_2N_2NiO_2$: C, 54.04; H, 6.80; N, 3.94. Found: C, 55.22; H, 7.32; N, 3.97.

General Procedure for the Attachment of the Linker to the Silica Support (14).[67] Caution! Mechanical stirring with a stirring bar should be avoided in the reactions involving silica as this destroys the fragile silica particles. Grace Davison silica 13 (4.0 g) was suspended in 20 mL of toluene, followed by the addition of trimethylaluminum (6.0 mL, 2 M solution in hexane). The reaction mixture was gently shaken manually at several intervals during a period of 1 h. The solvent was removed, and **14a** was washed three times with 20 mL of toluene and one time with 20 mL of pentane. Activated silica **14a** was dried in vacuo for 16 h at 20 °C.

General Procedure for the Synthesis of Silica-Supported Nickel Diimine Precatalysts (1−2).[67] Caution! Mechanical stirring with a stirring bar should be avoided in the reactions involving silica as this destroys the fragile silica particles. Linker silica support **14** was suspended in dichloromethane, and a solution of the nickel diimine complex **11**−**12** in dichloromethane was added at 20 °C. The reaction mixture was gently shaken manually at several intervals during a period of 1 h. The dichloromethane was removed after 1 h by pipet and filtered through a FTPE 0.45 μm filter as a sample preparation for the ICP-OES analysis. Silica-supported precatalysts **1**−**2** were washed three times with dichloromethane and dried in vacuo for 16 h at 20 °C. Amounts of silica, nickel diimine complex, and dichloromethane used in preparing supported catalysts via this procedure are given below.

Silica-Supported Precatalyst (1a): Theoretical Maximum Ni Loading of 1.0 wt %. Linker silica support **14a** (100 mg, Grace Davison XPO-2402, calcined at 200 °C), nickel diimine complex **11a** (17.5 mg), and 2 mL of dichloromethane were used. Precatalyst **1a** was isolated as a brown solid. ICP-OES analysis: 0.56 wt % Ni.

Silica-Supported Precatalyst (1b1): Theoretical Maximum Ni Loading of 1.0 wt %. Linker silica support **14a** (400 mg, Grace Davison XPO-2402, calcined at 200 °C), nickel diimine complex **11b** (56.4 mg), and 10 mL of dichloromethane were used. The dichloromethane solution removed after 1 h was colorless. Precatalyst **1b1** was isolated as a brown solid. ICP-OES analysis: 0.60 wt % Ni. Nickel loading based on the nickel content found in the dichloromethane solution after the support reaction: 0.99 wt % Ni.

Silica-Supported Precatalyst (1b1): Theoretical Maximum Ni Loading of 3.0 wt %. Linker silica support **14a** (100 mg, Grace Davison XPO-2402, calcined at 200 °C), nickel diimine complex **11b** (58.7 mg), and 12 mL of dichloromethane were used. The dichloromethane solution removed after 1 h had a red color. Precatalyst **1b1** was isolated as a brown solid. ICP-OES analysis: 2.0 wt % Ni.

Silica-Supported Precatalyst (1b2): Theoretical Maximum Ni Loading of 1.0 wt %. Linker silica support **14a** (2.0 g, Grace Davison SP9-496, calcined at 500 °C), nickel diimine complex (281 mg), and 25 mL of dichloromethane were used. The dichloromethane solution removed after 1 h had a weak-yellow color. Precatalyst **1b2** was isolated as a brown solid. Nickel loading based on the nickel content found in the dichloromethane solution after the support reaction: 0.99 wt % Ni.

Silica-Supported Precatalyst (1c2): Theoretical Maximum Ni Loading of 3.0 wt %. Linker silica support **14a** (200 mg, Grace Davison SP9-496, calcined at 500 °C), nickel diimine complex **11b** (117 mg), and 20 mL of dichloromethane were used. The dichloromethane solution removed after 1 h had a red color. Precatalyst

1b2 was isolated as a brown solid. Nickel loading based on the nickel content found in the dichloromethane solution after the support reaction: 2.8 wt % Ni.

Silica-Supported Precatalysts (1b3 and 1b4): Theoretical Maximum Ni Loading of 1.0 wt %. Linker silica support **14b** or **14c** (200 mg, Grace Davison SP9−496, calcined at 500 °C), nickel diimine complex **11b** (28.1 mg), and 10 mL of dichloromethane were used. Precatalysts **1b3** and **1b4** were isolated as brown solids.

Silica-Supported Precatalyst (1c): Theoretical Maximum Ni Loading of 1.0 wt %. Linker silica support **14a** (300 mg, Grace Davison SP9-496, calcined at 500 °C), nickel diimine complex **11c** (49.8 mg), and 10 mL of dichloromethane were used. The dichloromethane solution removed after 1 h was colorless. Precatalyst **1c** was isolated as a brown solid. Nickel loading based on the nickel content found in the dichloromethane solution after the support reaction: 1.0 wt % Ni.

Silica-Supported Precatalyst (1c): Theoretical Maximum Ni Loading of 2.0 wt %. Linker silica support **14a** (100 mg, Grace Davison SP9-496, calcined at 500 °C), nickel diimine complex **11c** (39.8 mg), and 10 mL of dichloromethane were used. The dichloromethane solution removed after 1 h had a brown color. Precatalyst **1c** was isolated as a brown solid. ICP-OES analysis: 1.33 wt % Ni.

Silica-Supported Precatalyst (2a1): Theoretical Maximum Ni Loading of 1.0 wt %. Linker silica support **14a** (100 mg, Grace Davison SP9-496, calcined at 500 °C), nickel diimine complex **12a** (11.6 mg), and 10 mL of dichloromethane were used. The dichloromethane solution removed after 1 h had a yellow color. Precatalyst **2a1** was isolated as a green/brown solid. Nickel loading based on the nickel content found in the dichloromethane solution after the support reaction: 0.98 wt % Ni.

Silica-Supported Precatalyst (2a2): Theoretical Maximum Ni Loading of 1.0 wt %. Linker silica support **14a** (100 mg, Grace Davison SP9-496, calcined at 600 °C), nickel diimine complex **12a** (11.6 mg), and 10 mL of dichloromethane were used. Precatalyst **2a2** was isolated as a deep-blue solid.

Silica-Supported Precatalyst (2a3): Theoretical Maximum Ni loading of 1.0 wt %. Linker silica support **14a** (100 mg, Grace Davison SP9-496, calcined at 700 °C), nickel diimine complex **12a** (11.6 mg), and 10 mL of dichloromethane were used. Precatalyst **2a3** was isolated as a deep-blue solid.

Silica-Supported Precatalyst (2b): Theoretical Maximum Ni Loading of 1.0 wt %. Linker silica support **14a** (100 mg, Grace Davison SP9-496, calcined at 500 °C), nickel diimine complex **12b** (13.7 mg), and 10 mL of dichloromethane were used. The dichloromethane solution removed after 1 h was colorless. Precatalyst **2b** was isolated as a green solid. Nickel loading based on the nickel content found in the dichloromethane solution after the support reaction: 0.99 wt % Ni.

Ethylene Polymerization. Polymerizations were carried out in a mechanically stirred 300 mL Parr reactor equipped with an electric heating mantle controlled by a thermocouple in the reaction mixture. The various procedures used for the polymerization are described below.

Procedure 1a. The reactor was charged with toluene and heated for 10 min at 100 °C. The hot toluene was removed, and the reactor was dried under vacuum for 10 min at 100 °C. After cooling to room temperature, the reactor was filled with argon. The reactor was then charged with 50 mL of pentane, followed by $Et_3Al_2Cl_3$ cocatalyst. A suspension of the supported precatalyst in 50 mL of pentane was cannula transferred to the reactor. All lines to the reactor were closed, and the temperature was raised to the required temperature within 5 min while stirring (350 rpm). The reactor was immediately pressurized with ethylene to the desired pressure after the desired temperature was reached, and the reaction mixture was stirred (350 rpm) for the desired time at the desired temperature. The temperature was controlled by cooling with water or heating with a heating mantle. The reaction mixture was cooled to 15 °C, and 20 mL of methanol was added. The polymer particles were isolated by filtration and dried in an oven at 75 °C. The filtrate was reduced in vacuo to check for the presence of oligomeric material.

Procedure 1b.[67] Modifications compared to procedure 1a. A solution of the cocatalyst in 100 mL of pentane was added to the reactor, followed by addition of the supported precatalyst. All lines to the reactor were closed, and the temperature was raised to the required temperature within 2 min while stirring (350 rpm).

Procedure 2. The reactor was charged with toluene and heated for 10 min at 100 °C. The hot toluene was removed, and the reactor was dried under vacuum for 10 min at 100 °C. After cooling to room temperature, the reactor was filled with ethylene. The reactor was then charged with 50 mL of pentane. A suspension of the supported precatalyst in 50 mL of pentane was cannula transferred to the reactor, followed by $Et_3Al_2Cl_3$ cocatalyst. The reactor was immediately pressurized with ethylene to the desired pressure, and the temperature was raised to the desired temperature within 5 min while stirring (350 rpm). The reaction mixture was stirred (350 rpm) for the desired time at the desired temperature. The temperature was controlled by cooling with water or heating with a heating mantle. The reaction mixture was cooled to 15 °C, and 20 mL of methanol was added. The polymer particles were isolated by filtration and dried in an oven at 75 °C. The filtrate was reduced in vacuo to check for the presence of oligomeric material.

Procedure 3. The reactor was charged with toluene and heated for 10 min at 100 °C. The hot toluene was removed, and the reactor was dried under vacuum for 10 min at 100 °C. After cooling to room temperature, the reactor was filled with argon. The reactor was charged with 50 mL of pentane. A suspension of the supported precatalyst in 50 mL of pentane was cannula transferred to the reactor, followed by $Et_3Al_2Cl_3$ cocatalyst. A small vacuum was applied, and the reactor was vented three times with ethylene. The reactor was immediately pressurized with ethylene to the desired pressure. The temperature was raised to the desired temperature within 5 min while stirring (350 rpm), and the reaction mixture was stirred (350 rpm) for the desired time at the desired temperature. The temperature was controlled by cooling with water or heating with a heating mantle. The reaction mixture was cooled to 15 °C, and 20 mL of methanol was added. The polymer particles were isolated by filtration, and dried in an oven at 75 °C. The filtrate was reduced in vacuo to check for the presence of oligomeric material.

Acknowledgment. We thank DuPont for financial support, D. J. Adelman, D. R. Loveday, S. D. Ittel, M. F. Schiffhauer, J. D. Citron, D. L. Kerbow, R. S. Schiffino, and A. M. A. Bennett (all of DuPont) and Prof. B. Rieger (University of Ulm) for helpful discussions, E. F. McCord (DuPont) for ^{13}C NMR analyses of PE samples, and E. Boyes (DuPont) for EDX analyses. Grace Davison is gratefully acknowledged for generous gifts of the silicas. Fellowship support was provided to P.P.P. by the Austrian Science Foundation (Erwin-Schroedinger-Stipendium, J 1917-CHE). Financial support was provided to H.S.S. by the Van Coeverden Adriani Foundation.

Supporting Information Available: X-ray crystallographic information file for **12a**. This material is available free of charge via the Internet at http://pubs.acs.org.

References and Notes

(1) Balsam, M.; Baum, P.; Engelmann, J. *Macromol. Mater. Eng.* **2001**, *286* (4), A7−A12.
(2) Peacock, A. J. *Polym. Mater. Sci. Eng.* **1999**, *80*, 291−292.
(3) Peacock, A. J. *Handbook of Polyethylene: Structure, Properties, and Applications*; Marcel Dekker: New York, 2000.
(4) Kaminsky, W.; Laban, A. *Appl. Catal., A* **2001**, *222*, 47−61.
(5) Wittcoff, H. A.; Reuben, B. G.; Plotkin, J. S. *Industrial Organic Chemicals*; John Wiley & Sons: New York, 2004.
(6) Ziegler, K.; Holzkamp, E.; Breil, H.; Martin, H. *Angew. Chem.* **1955**, *67*, 426.
(7) Wilke, G. *Angew. Chem., Int. Ed.* **2003**, *42*, 5000−5008.
(8) Bohm, L. L. *Angew. Chem., Int. Ed.* **2003**, *42*, 5010−5030.

(9) Fink, G.; Muelhaupt, R.; Brintzinger, H. H. *Ziegler Catalysts: Recent Scientific Innovations and Technological Improvements*; Springer: Berlin, 1995.
(10) Galli, P.; Vecellio, G. *Prog. Polym. Sci.* **2001**, *26*, 1287−1336.
(11) Weckhuysen, B. M.; Schoonheydt, R. A. *Catal. Today* **1999**, *51*, 215−221.
(12) Weckhuysen, B. M.; Wachs, I. E.; Schoonheydt, R. A. *Chem. Rev.* **1996**, *96*, 3327−3349.
(13) Reitz, W. In *Handbook of Polyethylene: Structure, Properties, and Applications*; Peacock A. J., Eds.; Marcel Dekker: New York, 2001; Vol. 16, pp 737−738.
(14) McKnight, A. L.; Waymouth, R. M. *Chem. Rev.* **1998**, *98*, 2587−2598.
(15) Coates, G. W. *Chem. Rev.* **2000**, *100*, 1223−1252.
(16) Scheirs, J.; Kaminsky, W. *Metallocene-Based Polyolefins*; John Wiley & Sons: New York, 2000; Vol. 1.
(17) Scheirs, J.; Kaminsky, W. *Metallocene-Based Polyolefins*; John Wiley & Sons: New York, 2000; Vol. 2.
(18) Ittel, S. D.; Johnson, L. K.; Brookhart, M. *Chem. Rev.* **2000**, *100*, 1169−1203.
(19) AlObaidi, F.; Ye, Z.; Zhu, S. *J. Polym. Sci., Part A: Polym. Chem.* **2004**, *42*, 4327−4336.
(20) Galland, G. B.; Quijada, R.; Rojas, R.; Bazan, G.; Komon, Z. J. A. *Macromolecules* **2002**, *35*, 339−345.
(21) Pettijohn, T. M.; Reagen, W. K.; Martin, S. J. (Phillips Petroleum Co.). U.S. Patent 5,331,070, priority date July 19, 1994.
(22) Mark, H. F.; Bikales, N. M.; Overberger, C. G.; Menges, G. *Encyclopedia of Polymers Science and Engineering*; John Wiley & Sons: New York, 1990.
(23) Musaev, D. G.; Morokuma, K. *Top. Catal.* **1999**, *7*, 107−123.
(24) Leatherman, M. D.; Svejda, S. A.; Johnson, L. K.; Brookhart, M. *J. Am. Chem. Soc.* **2003**, *125*, 3068−3081.
(25) Skupinska, J. *Chem. Rev.* **1991**, *91*, 613−48.
(26) Keim, W.; Hoffmann, B.; Lodewick, R.; Peuckert, M.; Schmitt, G.; Fleischhauer, J.; Meier, U. *J. Mol. Catal.* **1979**, *6*, 79−97.
(27) Keim, W.; Schulz, R. P. *J. Mol. Catal.* **1994**, *92*, 21−33.
(28) Vogt, D. In *Applied Homogeneous Catalysis with Organometallic Compounds*; Wiley-VCH: Weinheim, 1996; Vol. 1, pp 245−258.
(29) Johnson, L. K.; Killian, C. M.; Brookhart, M. *J. Am. Chem. Soc.* **1995**, *117*, 6414−15.
(30) Gates, D. P.; Svejda, S. A.; Onate, E.; Killian, C. M.; Johnson, L. K.; White, P. S.; Brookhart, M. *Macromolecules* **2000**, *33*, 2320−2334.
(31) Mecking, S. *Coord. Chem. Rev.* **2000**, *203*, 325−351.
(32) Schmid, M.; Eberhardt, R.; Klinga, M.; Leskelae, M.; Rieger, B. *Organometallics* **2001**, *20*, 2321−2330.
(33) Camacho, D. H.; Salo, E. V.; Ziller, J. W.; Guan, Z. *Angew. Chem., Int. Ed.* **2004**, *43*, 1821−1825.
(34) Brookhart, M. S.; Johnson, L. K.; Killian, C. M.; Arthur, S. D.; Feldman, J.; McCord, E. F.; McLain, S. J.; Kreutzer, K. A.; Bennett, M. A.; Coughlin, E. B.; Ittel, S. D.; Parthasarathy, A.; Tempel, D. J. (E. I. Du Pont de Nemours & Co. and University of North Carolina at Chapel Hill). Patent PCT WO9623010, priority date April 3, 1995.
(35) Small, B. L.; Brookhart, M.; Bennett, A. M. A. *J. Am. Chem. Soc.* **1998**, *120*, 4049−4050.
(36) Birtovsek, G. J. P.; Gibson, V.; Kimberley, B. S.; Maddox, P. J.; McTavish, S. J.; Solan, G. A.; White, A. J. P.; Williams, D. J. *Chem. Commun.* **1998**, *7*, 849−850.
(37) Bennett, A. M. A. (E. I. Du Pont de Nemours & Co.). Patent PCT WO9827124, priority date Dec 17, 1996.
(38) Britovsek, G. J. P.; Gibson, V. C.; Wass, D. F. *Angew. Chem., Int. Ed.* **1999**, *38*, 428−447.
(39) Gibson, V. C.; Spitzmesser, S. K. *Chem. Rev.* **2003**, *103*, 283−315.
(40) Svejda, S. A.; Johnson, L. K.; Brookhart, M. *J. Am. Chem. Soc.* **1999**, *121*, 10634−10635.
(41) Britovsek, G. J. P.; Bruce, M.; Gibson, V. C.; Kimberley, B. S.; Maddox, P. J.; Mastroianni, S.; McTavish, S. J.; Redshaw, C.; Solan, G. A.; Stroemberg, S.; White, A. J. P.; Williams, D. J. *J. Am. Chem. Soc.* **1999**, *121*, 8728−8740.
(42) Tempel, D. J.; Johnson, L. K.; Huff, R. L.; White, P. S.; Brookhart, M. *J. Am. Chem. Soc.* **2000**, *122*, 6686−6700.
(43) Cotts, P. M.; Guan, Z.; McCord, E.; McLain, S. *Macromolecules* **2000**, *33*, 6945−6952.
(44) Galland, G. B.; De Souza, R. F.; Mauler, R. S.; Nunes, F. F. *Macromolecules* **1999**, *32*, 1620−1625.
(45) Guan, Z.; Cotts, P. M.; McCord, E. F.; McLain, S. J. *Science* **1999**, *283*, 2059−2062.
(46) Moehring, V. M.; Fink, G. *Angew. Chem.* **1985**, *97*, 982−984.
(47) Schubbe, R.; Angermund, K.; Fink, G.; Goddard, R. *Macromol. Chem. Phys.* **1995**, *196*, 467−478.
(48) Kunrath, F. A.; Mota, F. F.; Casagrande, O. L., Jr.; Mauler, R. S.; de Souza, R. F. *Macromol. Chem. Phys.* **2002**, *203*, 2407−2411.
(49) Hlatky, G. G. *Chem. Rev.* **2000**, *100*, 1347−1376.
(50) Chien, J. C. W. *Top. Catal.* **1999**, *7*, 23−36.
(51) Kristen, M. O. *Top. Catal.* **1999**, *7*, 89−95.
(52) Fink, G.; Steinmetz, B.; Zechlin, J.; Przybyla, C.; Tesche, B. *Chem. Rev.* **2000**, *100*, 1377−1390.
(53) Mackenzie, P. B.; Moody, L. S.; Killian, C. M.; Lavoie, G. G. (Eastman Chemical Company). Patent PCT WO9962968, priority date Jan 22, 1998.
(54) Simon, L. C.; Patel, H.; Soares, J. B. P.; De Souza, R. F. *Macromol. Chem. Phys.* **2001**, *202*, 3237−3247.
(55) AlObaidi, F.; Ye, Z.; Zhu, S. *Macromol. Chem. Phys.* **2003**, *204*, 1653−1659.
(56) Vaughan, G. A.; Canich, J. A. M.; Matsunaga, P. T.; Gindelberger, D. E.; Squire, K. R. (Exxon Chemical Patents, Inc.). Patent PCT WO9748736, priority date June 17, 1996.
(57) Peruch, F.; Cramail, H.; Deffieux, A. *Macromolecules* **1999**, *32*, 7977−7983.
(58) Arthur, S. D.; Teasley, M. F.; Kerbow, D. L.; Fusco, O.; Dall'Occo, T.; Morini, G. (E. I. Du Pont de Nemours & Co. and Basell Technology Company B.V.). Patent PCT WO0168725, priority date March 9, 2000.
(59) Bansleben, D. A.; Connor, E. F.; Grubbs, R. H.; Henderson, J. I.; Younkin, T. R.; Nadjadi, A. R., Jr. (Cryovac, Inc.). Patent PCT WO0056786, priority date March 17, 1999.
(60) Bansleben, D. A.; Connor, E. F.; Grubbs, R. H.; Henderson, J. I.; Younkin, T. R.; Nadjadi, A. R., Jr. (Cryovac, Inc.). Patent PCT WO0056787, priority date March 17, 1999.
(61) Haddleton, D. M.; Radigue, A.; Kukulj, D.; Duncalf, D. (University of Warwick). Patent PCT WO9928352, priority date Dec 2, 1998.
(62) Boussie, T. R.; Murphy, V.; Hall, K. A.; Coutard, C.; Dales, C.; Petro, M.; Carlson, E.; Turner, H. W.; Powers, T. S. *Tetrahedron* **1999**, *55*, 11699−11710.
(63) Mendez Llatas, L.; Munoz-Escalona, L. A.; Campora Perez, J.; Carmona Guzman, E.; Lopez Reyes, M. (Repsol Quimica S.A.) European Patent EP 1134225, priority date March 13, 2000.
(64) Nesterov, G. A.; Zakharov, V. A.; Fink, G.; Fenzl, W. *J. Mol. Catal.* **1991**, *69*, 129−136.
(65) Kaul, F. A. R.; Puchta, G. T.; Schneider, H.; Bielert, F.; Mihalios, D.; Herrmann, W. A. *Organometallics* **2002**, *21*, 74−82.
(66) Mendez Llatas, L.; Munoz-Escalona, L. A.; Campora Perez, J.; Carmona Guzman, E.; Lopez Reyes, M. (Repsol Quimica S.A.). European Patent EP 1134236, priority date Mar 13, 2000.
(67) Preishuber-Pflugl, P.; Brookhart, M. *Macromolecules* **2002**, *35*, 6074−6076.
(68) Preishuber-Pflugl, P. (E. I. Du Pont de Nemours & Co. and University of North Carolina at Chapel Hill). Patent PCT WO02079276, priority date March 28, 2001.
(69) Interestingly, both the *E*,*E*- and *E*,*Z*-isomer of α-diimine **8b** were observed at room temperature by NMR spectroscopy. Rates and the mechanism of interconversion of these isomers can be determined by variable temperature NMR analysis. An NMR study of the dynamic behavior of α-diimine ligands will be reported separately.
(70) Teasley, M. F.: (E. I. Du Pont de Nemours & Co.). Patent PCT WO0022007, priority date Oct 13, 1999.
(71) Zheng, X.; Smit, M.; Chadwick, J. C.; Loos, J. *Macromolecules* **2005**, *38*, 4673−4678.
(72) AlObaidi, F.; Ye, Z.; Zhu, S. *Polymer* **2004**, *45*, 6823−6829.
(73) Knoke, S.; Ferrari, D.; Tesche, B.; Fink, G. *Angew. Chem., Int. Ed.* **2003**, *42*, 5090−5093.
(74) McKenna, T. F.; Soares, J. B. P. *Chem. Eng. Sci.* **2001**, *56*, 3931−3949.
(75) Ha, K.-S.; Yoo, K.-Y.; Rhee, H.-K. *J. Appl. Polym. Sci.* **2001**, *79*, 2480−2493.
(76) Still, W. C.; Kahn, M.; Mitra, A. *J. Org. Chem.* **1978**, *43*, 2923−2925.
(77) Daugulis, O.; Brookhart, M. *Organometallics* **2002**, *21*, 5926−5934.
(78) Tom Dieck, H.; Svoboda, M.; Greiser, T. *Z. Naturforsch., B: Chem. Sci.* **1981**, *36*, 823−832.
(79) McCloskey, J. A.; White, E. V. *J. Org. Chem.* **1970**, *35*, 4241−4244.
(80) Hon, Y.-S.; Chang, F.-J.; Lu, L.; Lin, W.-C. *Tetrahedron* **1998**, *54*, 5233−5246.
(81) Pangborn, A. B.; Giardello, M. A.; Grubbs, R. H.; Rosen, R. K.; Timmers, F. J. *Organometallics* **1996**, *15*, 1518−1520.
(82) Lu, Z.-l.; Mayr, A.; Cheung, K.-K. *Inorg. Chim. Acta* **1999**, *284*, 205−214.
(83) Kim, Y. H.; Kim, T. H.; Lee, B. Y.; Woodmansee, D.; Bu, X.; Bazan, G. C. *Organometallics* **2002**, *21*, 3082−3084.

MA061032V

CDV